buildings

MDPI

Article

Effects of Transverse Reinforcement Detailing on the Damage Mechanisms of RC Elements: Lessons from the 2023 Kahramanmaraş Earthquakes

Fatih Avcil [1,*], Dorin Radu [2], Ehsan Harirchian [3,*], Ercan Işık [1], Enes Arkan [4], Aydın Büyüksaraç [5] and Marijana Hadzima-Nyarko [6]

1 Department of Civil Engineering, Bitlis Eren University, Bitlis 13100, Türkiye; eisik@beu.edu.tr
2 Faculty of Civil Engineering, Transilvania University of Braşov, 500152 Brasov, Romania; dorin.radu@unitbv.ro
3 Institute of Structural Mechanics (ISM), Bauhaus-Universität Weimar, 99423 Weimar, Germany
4 Department of Architecture, Bitlis Eren University, Bitlis 13100, Türkiye; earkan@beu.edu.tr
5 Çan Vocational School, Çanakkale Onsekiz Mart University, Çanakkale 17400, Türkiye; absarac@comu.edu.tr
6 Faculty of Civil Engineering and Architecture Osijek, Josip Juraj Strossmayer University of Osijek, Vladimira Preloga 3, 31000 Osijek, Croatia; mhadzima@gfos.hr
* Correspondence: favcil@beu.edu.tr (F.A.); ehsan.harirchian@uni-weimar.de (E.H.)

Abstract

The twin earthquakes (Mw = 7.7 and Mw = 7.6) that struck Kahramanmaraş on 6 February 2023 caused severe damage to reinforced concrete (RC) buildings in southeastern Türkiye. Field observations showed that concrete quality and transverse reinforcement details have a major influence on the shear resistance of RC columns and beams. These factors also affect the fracture behaviour and structural integrity of the elements. The surveys revealed several common deficiencies. These included excessive transverse reinforcement spacing, insufficient bar diameters, inadequate hook details, low-quality materials, and poor workmanship. The lack of seismic design principles or their improper implementation further increased the level of damage observed in the buildings. In this study, reinforcement-induced failure in columns and beams was evaluated in detail and observationally in the context of seismic and structural engineering. The main novelty of this work is the direct integration of these in situ post-earthquake field assessments with comprehensive 3D non-linear static simulations of 20 distinct structural models. Variations in parameters such as tie spacing, rebar diameter, bend angle of hooks, and structural material strength were numerically investigated through these models. It was determined that mechanisms close to fracture occurred, especially in columns, owing to deficient concrete compressive strength and transverse reinforcement deficiencies. Findings show that an upgrade in column shear capacity of up to 10% is achievable by reducing the spacing from 300 mm to 200 mm, whereas the implementation of a 135° hook anchorage substantially restrains the buckling of longitudinal reinforcement. As a key practical contribution, this study also proposes a specific FRP retrofitting design that successfully restores the lost shear capacity in all deficient columns. This blended field-and-computational strategy offers actionable, data-backed guidance for engineering design, the optimization of building regulations, and the identification of rehabilitation priorities in highly active seismic zones.

Keywords: earthquake; structural integrity; Kahramanmaraş; RC; reinforcement

Check for updates

Academic Editor: Flavio Stochino

Received: 27 June 2026
Revised: 16 July 2026
Accepted: 20 July 2026
Published: 21 July 2026

1. Introduction

Ensuring the structural robustness of legacy reinforced concrete (RC) structures is a major challenge in seismically vulnerable areas, especially for assets developed before the implementation of contemporary seismic design rules. A significant majority of these substandard structures suffer from critical flaws such as low-strength concrete, deficient confinement, and plain reinforcement. These deficiencies, along with structural irregularities, severely impair the ductility and shear resistance of structural components, promoting premature brittle failures under seismic excitation. Moreover, these vulnerabilities stem not only from outdated regulatory frameworks but are also critically driven by poor workmanship and construction errors [1–6]. To make these weak buildings safer, different strengthening and retrofitting methods are widely used [7–11]. These methods are necessary to prevent sudden collapse during earthquakes.

Material and detailing inadequacies in reinforced concrete elements fundamentally compromise structural robustness by modifying internal stress distributions and triggering premature non-ductile failure. The compounding effect of these vulnerabilities restricts the displacement capacity of RC components while catalyzing fracture modes that endanger global structural equilibrium. Imperfections originating from reinforcement and concrete in RC structural elements disrupt stress distribution, facilitating crack initiation and propagation, and thus having a decisive impact on the structure's fracture behavior. Because such imperfections weaken the overall performance of the material, addressing the fracture process within the scope of engineering damage mechanics is crucial for accurately assessing structural integrity. Therefore, the reliability of reinforced concrete elements necessitates a comprehensive analysis approach that considers the interaction of imperfections with fracture mechanisms. Transverse reinforcement detailing and material properties in RC elements play a critical role in ensuring structural stability, being among the most fundamental parameters determining the nature of crack initiation and crack propagation. Particularly in elements subject to dominant shear forces, the amount and placement of transverse reinforcement, hook detail, and the size of the densification zone directly shape the crack initiation threshold, crack propagation direction, and the conditions for the activation of brittle fracture behavior. Inadequate transverse reinforcement arrangements have the potential to result in sudden shear failure, concrete cover stripping, and element-level integrity loss. This demonstrates that the overall performance of a structural system depends not only on material strength but also on detailing strategies, which must be considered from a damage mechanics perspective [12–21]. A broader perspective on the impact of transverse reinforcement on damage behavior in RC structural members will fill a considerable gap in the current literature. This study combines aha data from the 2023 earthquakes with three-dimensional numerical models to provide a comprehensive analysis of the shear-based failure mechanisms of RC members.

The Kahramanmaraş earthquake couple, which caused catastrophic failure across 11 provinces in Türkiye and occurred 9 h apart on 6 February 2023. The initial seismic event, registering a moment magnitude (M_w) of 7.7, struck on 6 February 2023 at 04:17 local time, centered in Kahramanmaraş-Pazarcık and lasted approximately 75 s. The second seismic event, with a magnitude of 7.6, hit Kahramanmaraş-Elbistan at 13:24 on the same day and lasted nearly 25 s. As of 22 March 2023, the region had experienced heightened seismic activity, registering more than 10,000 subsequent tremors following the primary events according to official seismic monitoring data as of 22 March 2023. The critical significance of the design and construction phases of structural components is underscored by the varying degrees of damage, fracture, and collapse observed in RC buildings post-earthquake. Türkiye has suffered severe casualties and extensive property damage as a result of both instrumental and historical earthquakes. Regula-

https://doi.org/10.3390/buildings16142897

tions regarding these structures are being developed in Türkiye, taking into account the damage to RC structures resulting from these earthquakes. Following the earthquakes, necessary lessons have been learned over time, and important steps have been taken in terms of both seismic hazard maps and the development of earthquake design codes. However, the lack of due care, especially during the construction phase, has caused the structures' seismic performance to be lower than anticipated in their projects. The catastrophic events in Kahramanmaraş served as a stark reminder of these structural deficiencies. These consecutive earthquakes negatively affected the damage levels of the structures and increased the destructiveness of the seismic event. Consequent to the earthquake, significant destruction and structural failure occurred, especially in RC structures, representing the most prevalent building typology within urban environments. The primary cause of the damage was the lack of or complete application of earthquake-resistant structural design criteria [22–27].

Assessing structural damage following earthquakes of varying magnitudes and intensities is essential for maintaining the continuity of social life, accurately evaluating seismic risk in inhabited areas, and improving structural design regulations. Information obtained from post-earthquake damage investigations provides a valuable basis for advancing both earthquake engineering and structural engineering research. Furthermore, damage assessments play a crucial role in determining whether buildings have been designed and constructed in compliance with seismic design principles. Evidence from numerous post-earthquake investigations in Türkiye consistently indicates that inadequate transverse and longitudinal reinforcement in RC structural members, together with the use of low-strength concrete, are among the primary factors contributing to structural failure [28–44]. In the studies examining the seismic damage in RC structures following the recent Kahramanmaraş seismic events, failures caused by structural irregularities came to the fore, while reinforcement and concrete properties were again revealed to be one of the main factors. Previous research has shown that insufficient transverse reinforcement in RC structural members is unable to provide adequate resistance against the shear forces generated during earthquakes, resulting in various levels of structural damage. Although these studies provide valuable comparisons of the seismic design requirements introduced in different editions of earthquake codes, they generally do not incorporate detailed structural analyses to evaluate the in situ performance of buildings under seismic event loading [45–56].

To prevent failure from the internal forces that will occur due to earthquakes in structural elements, it has been suggested to use transverse reinforcements and special earthquake crossties for confinement purposes, and the method of application has found its place in earthquake codes [57,58]. Transverse reinforcements, which are sized to resist the shear forces that will occur in beams and columns with concrete, can be exposed to faulty or incomplete applications, especially during the construction phase. Vulnerabilities driven by inadequate confinement due to wide stirrup spacing, combined with substandard concrete compressive strength, lack of interlocking between reinforcements, and insufficient RC cover thickness, can cause failure of these elements. In this context, it is important to select the spatial configuration and quantity of both transverse ties and longitudinal rebars within the columns and beams, following the respective standards and codes to place these elements into the structure during the actual execution phase.

Studies on structural RC elements under the effect of seismic events are intended to increase the structural load capacity of these members by preventing damage or collapse. Field investigations by the authors revealed that many collapsed or heavily damaged structures suffered from deficient transverse reinforcement in columns and beams, including excessive spacing, inadequate diameter, poor anchorage detailing, and corrosion. Numerous investigations have focused on evaluating the effects of the transverse and longitudinal reinforcement changes in RC load-bearing elements on structural performance. In his study, Çolakoğlu [59] tried to reveal the influence of confinement tie spacing as a variable in RC structures on structural performance. Atar et al. [60] examined the failure caused by transverse reinforcement in RC columns in an earthquake region. Merter and Uçar [61] examined the effect of longitudinal and transverse reinforcement conditions in RC structures on different variables. Taşkın and Okay [62] examined the impact of transverse reinforcement type on the structural response of RC columns. İnel et al. [63] examined the earthquake performance of RC structures with various stories and took into account the transverse reinforcement spacing as a variable. Işık [64] examined the effect of special earthquake crossties used in columns on structural performance. İnel et al. [65] considered the effects of changes in transverse reinforcement spacing, as well as other variables, while evaluating the structural response of 14 RC structures under earthquake effects. Fortney et al. [66] conducted experimental tests to quantify the impact of transverse reinforcement in beams on structural performance. Ding et al. [67] assessed the consequences of high-strength concrete and reinforcement on axial compression. Mangalathu et al. [68] tried to determine the shear forces in slabs without transverse reinforcement by machine learning. Tripathi and Dhakal [69] investigated the effects of transverse reinforcement conditions on buckling in rectangular-section RC shear walls. Colajanni et al. [70] theoretically investigated the effect of transverse reinforcement with different slopes on the shear force capacities of RC beams. Sucharda [71] investigated the ultimate Shear resistance of RC beam elements without stirrup reinforcements in detail. Goharrokhi et al. [72] experimentally studied the consequences of corrosion on the confinement efficiency and the resulting axial compressive capacity of structural elements. In this context, building accurate numerical models is critical for evaluating existing RC structures. We need reliable simulation tools to predict how these buildings behave under seismic loads before applying any retrofitting methods [73–76]. This modeling approach is essential to identify structural weaknesses and design effective retrofitting or strengthening solutions.

Although previous studies have highlighted these structural deficiencies, only a limited number have integrated field-based photographic documentation with numerical analyses to quantitatively determine the influence of individualized parameters on shear strength and structural ductility. In this study, an overview of the Kahramanmaraş earthquakes is first presented to establish the context of the investigation. Subsequently, damage resulting from inadequate transverse reinforcement in reinforced concrete (RC) columns and beams was examined through field observations conducted by the authors in the earthquake-affected provinces. The observed failure mechanisms associated with different transverse reinforcement configurations were then analyzed separately for columns and beams to evaluate their respective structural responses. To evaluate the structural implications of various transverse reinforcement conditions on columns and beams, different variables were used in the RC structure model, and their effects on the structural performance were investigated. The numerical assessment was carried out via static pushover analysis, in which several parameters were considered as variables. These parameters included the diameter and spacing of transverse reinforcement, the type of reinforcing steel, the use of low-strength concrete, the presence of special seismic crossties in columns, differences in the material properties of transverse and longitudinal reinforcement, and the bending angles of transverse reinforcement. While five different selections were made for transverse reinforcement spacing in columns: 100, 200, 300, 400, and 500 mm, three different selections were made as Φ8, Φ10, and Φ12 for transverse reinforcement diameter. For the hook angle of transverse reinforcement in columns, two variables were used: 90° and 135°. S220 and S420 steel grades were used as variables for transverse and longitudinal reinforcement materials. In addition, structural analyses were also performed separately for the use of crossties and diamond stirrups in columns. Three different reinforcement spacing values, two different angle values, and two different transverse reinforcement diameters were varied across the investigated RC beams. To investigate the impact of low-strength concrete on the seismic behavior of the structure, supplementary structural analyses were carried out by adopting a concrete strength class of C8/10 concrete. Following the structural evaluations executed individually for each distinct parameter, shear forces and target displacement values were obtained, and comparisons were made. To show the effect of each variable more clearly, other structural characteristics were kept constant. The obtained results were in comparison to the values estimated in the preceding in the last two earthquake codes used in Türkiye, and comments and suggestions were made. Unlike previous studies, this research provides a more comprehensive assessment of damage resulting from inadequate transverse reinforcement in reinforced concrete columns and beams by integrating detailed structural analyses with the evaluation of observed failure mechanisms. The novelty of this work lies in integrating large-scale field data with parameter-controlled numerical analyses to produce actionable recommendations for design, construction, and retrofit. By combining post-earthquake observations with detailed structural analyses, this research contributes to the integration of earthquake engineering practice and seismic code development. The findings provide a scientific basis for improving the structural safety, seismic performance, and overall integrity of reinforced concrete (RC) structures.

2. Tectonic Dynamics and Seismic Activity in Eastern Anatolia and 2023 Kahramanmaraş Earthquakes

The tectonic dynamics of Türkiye, particularly in Eastern Anatolia, are shaped by the interaction of the Arabian, Eurasian, and Anatolian Plates. The tectonic regime of this region is dominated by compressional forces generated by the northward convergence of the Arabian Plate, which drives the westward displacement of the Anatolian Plate (Figure 1). The regional deformation is primarily accommodated by two major active fault systems: The North Anatolian Fault Zone (NAFZ) and the East Anatolian Fault Zone (EAFZ), which are central to this tectonic activity. The EAF, extending about 580 km, is notable for its high seismicity, with a history of significant earthquakes. Major historical events include the 1114 Kahramanmaraş Earthquake (M > 7.8) and the 1822 Halep Earthquake (M = 7.5), among others. In the instrumental period, the region has experienced various earthquakes, such as the 2020 Elazığ earthquake (M_w = 6.8). While these events have been impactful, they generally did not reach the catastrophic levels of earlier historical earthquakes. The EAFZ is characterized as a left-lateral strike-slip fault, with destructive earthquakes occurring along its length, particularly in its central and southwest sections. This fault, along with the Dead Sea Fault Zone (DSFZ), profoundly influences the seismic hazard profile of the region. The historical record shows a pattern of catastrophic earthquakes concentrated in specific areas, particularly where the EAFZ meets the NAFZ in Karlıova [77–79]. Interestingly, the Gölbaşı-Türkoğlu stretch of the EAF has not experienced a major earthquake in the last 500 years, indicating a period of seismic quiescence. This behavior suggests that while the fault is currently locked, the potential for future significant seismic events remains, underscoring the importance of continuous monitoring and research in this tectonically active area.

https://doi.org/10.3390/buildings16142897

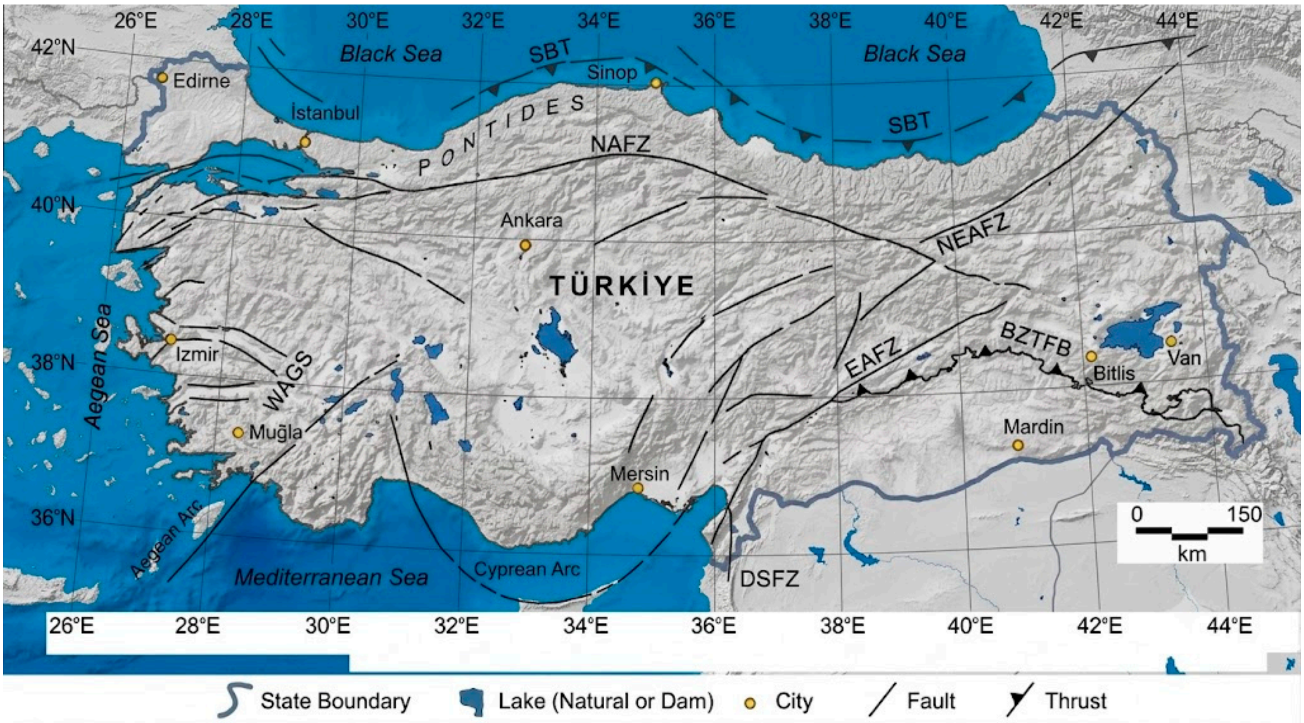

Figure 1. Tectonic map of Türkiye [80].

The Kahramanmaraş region experienced unprecedented doublet earthquakes on 6 February 2023, generating sequential shocks of M_w = 7.7 and M_w = 7.6 merely nine hours apart. These events began a series of significant earthquakes, which soon included M_L = 5.7, M_w = 6.0, M_w = 6.4, and M_w = 6.6 magnitudes. These earthquakes caused widespread devastation throughout 11 provinces, leading to the deaths of more than 50,000 people, injuries to over 100,000 individuals, and the loss of habitability in more than 500,000 residential buildings. Information about the magnitudes, locations, and focal depths of both earthquakes has been summarized in Table 1, based on data from AFAD (Çankaya, Türkiye) [81] and USGS (Reston, VA, USA) [82].

Table 1. Data obtained from different sources regarding the 2023 Kahramanmaraş earthquakes.

Date/Time	Coordinate	Location	Magnitude (M_w)	Depth (km)	Source
06.02.2023 04:17:34 (TSI)	37.288° N, 37.043° E	Kahramanmaraş (Pazarcık)	7.7	8.60	AFAD
	37.225° N, 37.021° E		7.8	10.0	USGS
06.02.2023 13:24:47 (TSI)	38.089° N, 37.239° E	Elbistan-Ekinözü (Kahramanmaraş)	7.6	7.0	AFAD
	38.024° N, 37.203° E		7.5	10	USGS

The distances of the epicentral distances of these regions from the primary seismic source are as follows: Kahramanmaraş 52 km, Gaziantep 23 km, Kilis 45 km, Osmaniye 76 km, İskenderun (Hatay) 101 km, Adıyaman 122 km, Malatya 169 km, Antakya (Hatay) 130 km, and Diyarbakır 282 km. The distances of these provinces from the second earthquake are Kahramanmaraş 70 km, Gaziantep 110 km, Malatya 112 km, Adıyaman 114 km, Osmaniye 147 km, Kilis 150 km, İskenderun (Hatay) 198 km, Antakya (Hatay) 237 km, and

Diyarbakır 274 km. The estimated intensity maps for both earthquakes obtained by AFAD are shown in Figure 2.

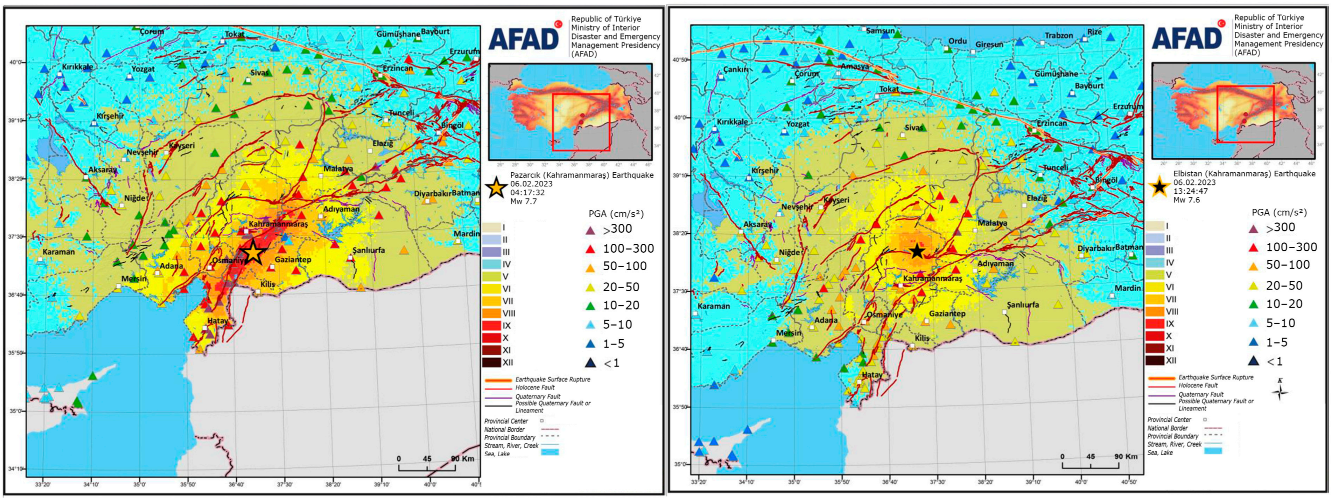

M_w= 7.7 Pazarcık (Kahramanmaraş) M_w= 7.6 Elbistan (Kahramanmaraş)

Figure 2. Earthquake intensity maps [81].

The earthquakes on 6 February 2023 struck the Pazarcık and Elbistan districts of Kahramanmaraş province, in an area where the EAFZ had been inactive for approximately 500 years. These earthquakes resulted in substantial loss of life and property across 11 provinces in Türkiye, and their effects were also felt significantly in neighboring regions. Additionally, the tremors caused casualties and damage in Syria, with over 50,000 fatalities reported in Türkiye alone. Figure 3 illustrates Türkiye's primary tectonic features and the epicenters of the 6 February 2023 earthquakes.

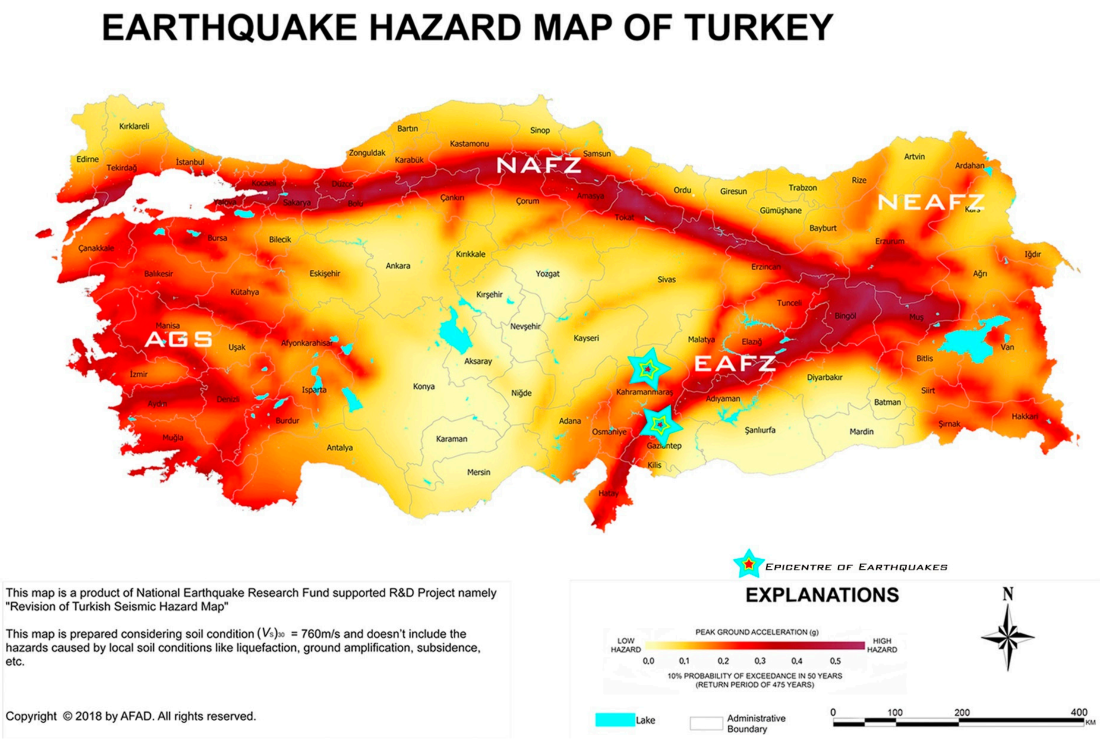

Figure 3. Earthquake hazard map of Türkiye and epicenters of the 6 February 2023 earthquakes (Adopted from AFAD, 2025 [83]).

3. Failure Mechanisms Associated with Transverse Reinforcement in RC Structures

Factors including the event magnitude, local ground conditions, and structural system features play pivotal roles in shaping seismic damage. One of the main causes of failure, fracture, or collapse in RC structures is the properties and conditions of the concrete and reinforcement used in RC. RC represents a composite structural medium formulated by blending concrete and reinforcement. If one of these is insufficient or missing, and the adhesion between them is inadequate, it adversely affects the seismic performance of RC structures [84,85]. The utilization of low-grade concrete alongside inadequate longitudinal/transverse bar ratios and substandard confinement steel directly affects structural damage or fracture. Deficiencies in reinforcement can increase the level of structural damage, especially in columns, beams, and shear walls. The amount, spacing, and arrangement of transverse and longitudinal reinforcement should comply with the relevant codes and standards. Proper detailing and correct placement during construction help reduce earthquake damage. After major earthquakes, buildings with different structural systems have shown different levels of damage, ranging from minor damage to complete collapse. In RC structures, insufficient spacing of transverse reinforcement in columns and shear walls led to varying degrees of damage. The primary function of the longitudinal reinforcements used in structural elements like columns, beams, and shear walls is to resist shear forces, which are expected from the transverse reinforcements placed perpendicularly. Additionally, transverse reinforcements help maintain the position and arrangement of the longitudinal reinforcements by interlocking them. Proper transverse reinforcement spacing delays the buckling of longitudinal reinforcement. It also confines the core concrete and improves its behavior. This increases the concrete strength and enhances the ductility of the structural member. Insufficient use of transverse reinforcements adversely affects many of these expected functions. Observational studies in the seismic event-affected region revealed that non-compliance with design rules regarding transverse reinforcements resulted in significant structural failure.

3.1. Structural Vulnerabilities Related to Transverse Reinforcement Detailing in RC Columns

The lack of sufficient transverse reinforcement in RC columns, beams, and beam–column joints has adversely affected the seismic performance expected from these structural components. Figure 4 summarizes the transverse reinforcement provisions for columns prescribed in the two latest earthquake design codes implemented in Türkiye.

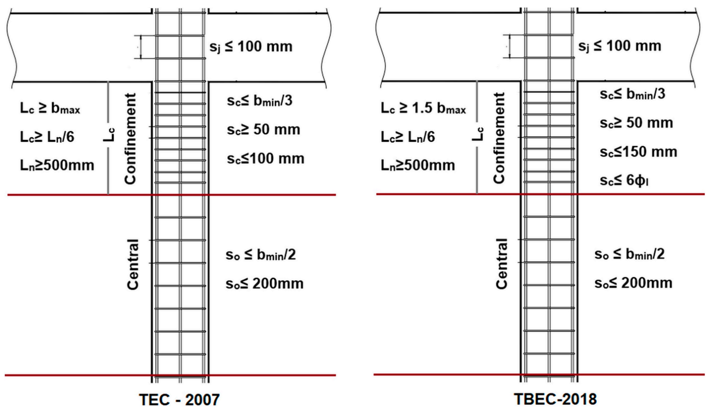

Figure 4. The shear and confinement detailing rules for columns in accordance with the 2007 and 2018 Turkish Seismic Design Codes [53,54].

The structural damage typologies documented in this section represent various distinct mid-rise reinforced concrete (RC) buildings. These structures, situated across the most severely earthquake-affected provinces of Hatay, Kahramanmaraş, and Adıyaman, were predominantly constructed before the year 2000. Most of the inspected buildings fell under the category of heavy damage, while the remainder experienced complete collapse. Systematic field evaluations revealed critical common structural and material deficiencies among these buildings: the measured transverse reinforcement (stirrup) spacing was significantly wider than the limits prescribed by seismic design codes, the hook details were overwhelmingly configured at 90°, and the concrete compressive strengths were critically below standard design requirements. In RC systems, columns and beams constitute the primary load-bearing elements of the structural system. The beam–column connections play a critical role in transferring loads between horizontal and vertical members. Within RC frame structures, these joint regions are subjected to significant shear demands under seismic loading, which can have a decisive influence on overall earthquake resistance. Earthquake-induced forces generate concentrated shear stresses at these connections, often leading to localized deterioration of concrete. This problem can be alleviated through the provision of adequate transverse reinforcement in the beam-column joint regions. Nevertheless, Figure 5 illustrates cases of concrete crushing and buckling of longitudinal reinforcement resulting from insufficient transverse reinforcement at these connections.

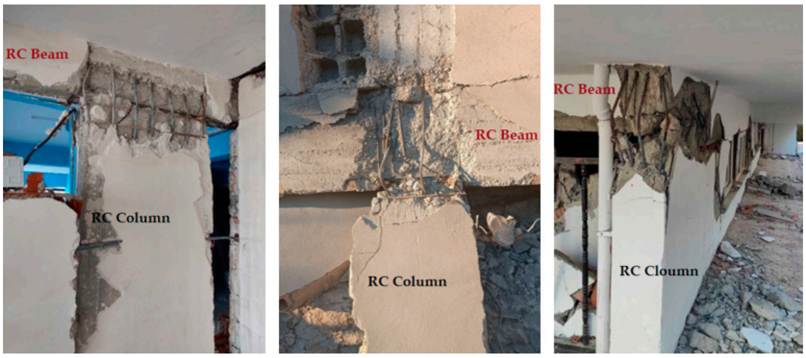

Figure 5. Illustrations of structural failure modes, characterized by the simultaneous crushing of the concrete matrix and lateral buckling of longitudinal bars due to inadequate stirrup configurations in beam-column joints.

After load transfer through the beam-column joints, bending moments increase at the top of the columns, especially during earthquakes. This may cause damage in the plastic hinge regions. Figure 6 shows the plastic hinges formed at the column ends due to inadequate transverse reinforcement and the resulting damage. In these regions, insufficient confinement provided by transverse reinforcement relative to seismic code requirements results in buckling of longitudinal reinforcement and consequently induces brittle failure of the surrounding concrete.

Figure 6. Representative failure modes observed at the upper confinement zone consequent to substandard transverse reinforcement detailing.

The damage examples resulting from insufficient and inadequate transverse reinforcement at the lower end region of the RC columns during the earthquake are shown in Figure 7.

Figure 7. Examples of failures in the lower end of the column.

Figure 8 illustrates representative failure modes in the mid-height region of the columns, triggered by the combination of deficient lateral confinement and low-grade concrete.

Figure 8. Failures in the middle region of the column.

Considering these damages, the codes used in Türkiye recommend increasing the transverse reinforcement in the lower and upper regions of columns. This aims to enhance the strength and ductility of these areas. However, excessive use of longitudinal reinforcement in these regions has caused issues with the expected contribution of transverse reinforcements to increasing the brittleness of the concrete. Examples of damage occurring in the column end sections are shown in Figure 9.

Figure 9. Examples of failures resulting from the failure of transverse reinforcements to perform their expected functions due to excessive use of longitudinal reinforcement.

Insufficient transverse reinforcement in short columns, which can form due to various reasons, increases the extent of damage in these structures. Examples of failure resulting from inadequate transverse reinforcement in short columns are shown in Figure 10.

Figure 10. Buckling of longitudinal reinforcement due to insufficient transverse reinforcement in short columns.

In damaged RC structures in earthquake-prone areas, the use of plain reinforcement has not been commonly observed. While previous regulations allowed the use of plain reinforcement until 2007, the regulations after 2007 permitted this type of reinforcement only in transverse and stirrups. Since plain reinforcement lacks any ribs, there is no mechanical bond formed between the concrete and the reinforcement. As a result, the concrete can easily slip off the reinforcement, preventing the concrete and reinforcement from working together, which contradicts the fundamental principle of reinforced concrete. During earthquake loading, the weak bond between plain reinforcement and concrete leads to early reinforcement slip and rapid bond deterioration. This behavior reduces the composite action between concrete and steel, resulting in concrete spalling and local damage. In contrast, the ribs present in deformed reinforcement significantly enhance the interlock between the concrete and the reinforcement. Examples of failure resulting from insufficient interlock between concrete and reinforcement due to the use of plain reinforcement are shown in Figure 11.

Figure 11. Insufficient concrete-reinforcement interlock resulting from the use of plain reinforcement.

A commonly observed type of failure resulting from insufficient transverse reinforcement is the buckling of longitudinal reinforcement. Buckled longitudinal reinforcement can lead to the crushing and spalling of concrete. Additionally, failures have been observed in transverse reinforcement when the shear force capacity is exceeded. Examples of buckling in longitudinal reinforcement and fractures in transverse reinforcement are shown in Figure 12. In cases where the transverse reinforcement in columns is insufficient, the transverse reinforcements may not prevent the buckling of longitudinal reinforcement, leading to fractures in the transverse reinforcements.

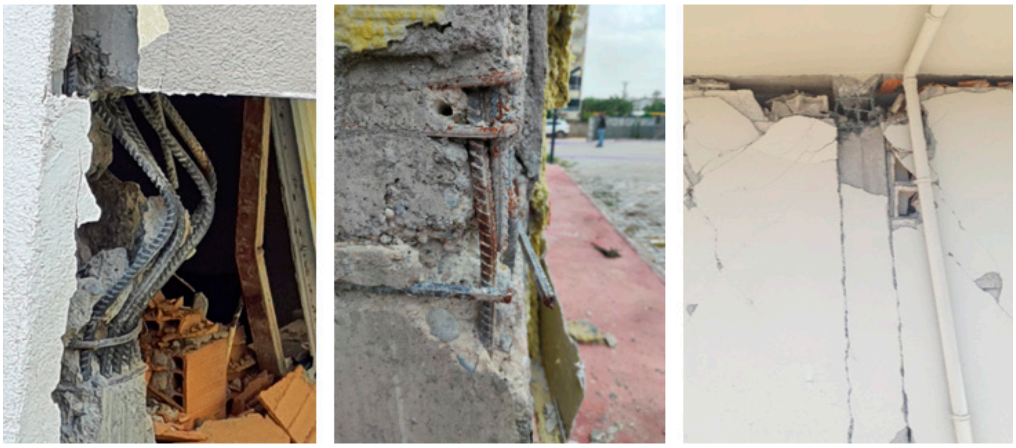

Figure 12. Buckling samples in longitudinal reinforcement.

One of the key parameters influencing the load-bearing capacity of RC structural elements is insufficient concrete cover thickness. Inadequate cover may lead to the corrosion of reinforcement over time, which reduces the effective cross-sectional area of steel and consequently diminishes the load-carrying capacity of the member. Examples of columns that experienced corrosion-induced damage because of insufficient concrete cover are presented in Figure 13.

Figure 13. Corroded reinforcement and insufficient interlock resulting from inadequate concrete cover thickness.

In addition to inadequate concrete cover thickness, insufficient transverse reinforcement also increases the level of damage. Examples of failure resulting from insufficient transverse reinforcement and clear concrete cover depth are shown in Figure 14.

Figure 14. Examples of failure from insufficient transverse reinforcement and concrete cover.

Due to insufficient transverse reinforcement, the load-bearing capacities of longitudinal reinforcements have been exceeded, resulting in fractures in the longitudinal reinforcements. The characteristics associated with this type of damage are clearly presented in Figure 15.

Figure 15. Fracture in the longitudinal reinforcement.

Shear forces that will occur in columns are supported by the contribution of the concrete as well as the transverse reinforcement. The failure manifestations arising from the combined presence of inadequate lateral confinement and low compressive strength concrete are illustrated in Figure 16.

Figure 16. Illustrations of seismic failure modes characterized by the simultaneous crushing of the concrete matrix and lateral buckling of longitudinal bars due to substandard material strength and detailing.

Although seismic design provisions recommend that transverse reinforcement in columns be detailed with 135° hooks around longitudinal reinforcement, in practice 90° hook configurations are sometimes used, which may result in inadequate anchorage of the transverse reinforcement. This detailing deficiency can facilitate the premature slip or pull-out of transverse reinforcement from the longitudinal bars. Examples of the resulting damage are presented in Figure 17.

However, transverse reinforcements applied at an angle of 135° have not slipped from the longitudinal reinforcements. An example of a 135° angle stirrup implementation is shown in Figure 18.

In RC structures, poor reinforcement workmanship is a significant factor affecting the expected functions of the reinforcements. Changes in the position and arrangement of the reinforcements can lead to an overload of load-bearing elements failing. Incorrect reinforcement placement changes how loads are transferred through the structural member.

This leads to stress concentrations, increasing the risk of cracking, concrete crushing, and local failure during an earthquake. Examples of damage caused by poor reinforcement workmanship are shown in Figure 19.

Figure 17. Examples of slips of transverse reinforcement caused by insufficient anchorage of 90° hooks during earthquake loading.

Figure 18. An example of a transverse reinforcement applied with a 135° angle.

Figure 19. Examples of failed RS columns caused by poor reinforcement workmanship and insufficient transverse reinforcement.

The combined structural performance of longitudinal and transverse reinforcement in reinforced concrete (RC) columns is adversely influenced when ribbed bars are used as longitudinal reinforcement together with plain bars as transverse reinforcement. This reinforcement configuration results in inadequate anchorage, thereby limiting the intended contribution of the reinforcement system under loading conditions. Typical failure mechanisms associated with RC columns incorporating ribbed longitudinal reinforcement and plain transverse reinforcement are illustrated in Figure 20.

Figure 20. Configuration of distinct reinforcement types in transverse and longitudinal directions.

3.2. Failures Caused by Transverse Reinforcement in RC Beams

In the updated Türkiye Building Earthquake Code (TBEC-2018) [54], the rules regarding the transverse reinforcements that should be used in beams are shown in Figure 21.

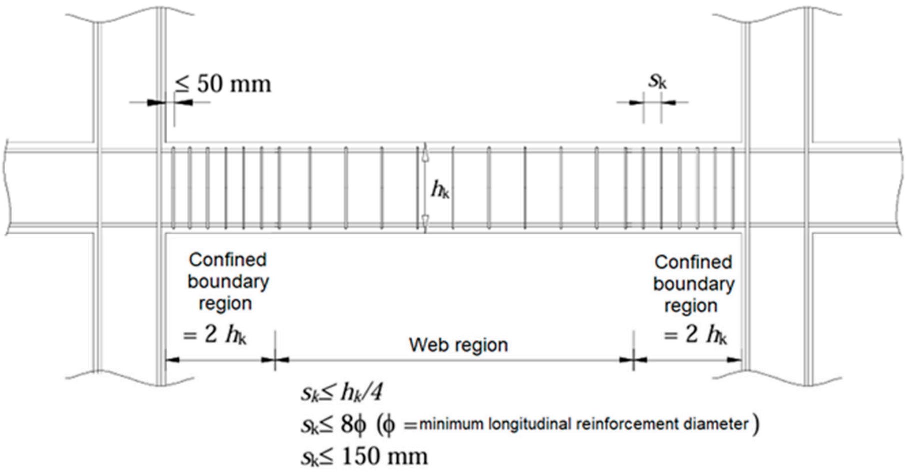

Figure 21. Design conditions for RC beams as prescribed in TBEC-2018 [54].

In RC beams, excessive use of longitudinal reinforcement negatively affects the bond between the concrete and the reinforcement. Excessive longitudinal reinforcement limits the spacing between bars, making concrete placement and compaction difficult. This often creates voids and a weak bond, which reduces the overall capacity of the member. Additionally, as with columns, insufficient concrete cover thickness impacts the load-carrying capacity of the reinforcements. An example of damage observed in a beam due to excessive longitudinal reinforcement and insufficient concrete cover thickness is shown in Figure 22.

Figure 22. Insufficient concrete cover thickness in the RC beam.

A lack of transverse reinforcement caused diagonal shear cracks to develop rapidly. As seismic demand grew, these cracks widened, reducing the beam's shear capacity and leading to brittle failure in some members. Examples of failure caused by insufficient transverse reinforcement in beams are shown in Figure 23.

Figure 23. Examples of failure caused by insufficient transverse reinforcement in beams.

The most significant damage caused by insufficient transverse reinforcement, similar to that in columns, is the buckling of longitudinal reinforcement. Examples of lateral buckling damage occurring in longitudinal reinforcement in beams are shown in Figure 24.

Figure 24. Lateral buckling failure in RC beams.

Corrosion reduces the steel's effective area and weakens its bond with concrete. In plain-bar members, this is highly critical; since there is already little mechanical interlock, cracking occurs earlier and load capacity drops. Examples of failure caused by the use of plain reinforcement and the corrosion of reinforcement in beams are shown in Figure 25.

Figure 25. Examples of failure caused by corroded plain reinforcement.

The use of different types of reinforcement in transverse and longitudinal bars in beams, similar to columns, has caused anchorage problems between the reinforcements. An example of this type of damage is shown in Figure 26.

Figure 26. The use of different types of reinforcement in longitudinal and transverse bars.

4. Numerical Analysis

A 6-story RC building model representative of common Turkish urban stock was analyzed using SeismoStruct-2025 [86]. Field survey data informed the choice of parameter ranges for transverse reinforcement spacing (100–500 mm), diameter (Φ8–Φ12), hook angle (90°/135°), and material grade (S220/S420). Beam and column cross-sections, concrete cover, and load patterns were based on typical TBEC-2018-compliant designs but deliberately varied to simulate non-compliant cases observed in the field. Boundary conditions assumed fixed supports at the foundation level and distributed gravity loads corresponding to residential occupancy. Pushover analyses were conducted in both principal directions to determine shear capacity exceedance and target displacement.

4.1. Numerical Analysis for the Entire Structural Model

Based on post-earthquake field investigations and the observed structural damage, the spacing of transverse reinforcement can be identified as one of the principal factors influencing the seismic performance of reinforced concrete members. To evaluate this effect, a series of structural analyses was conducted on a representative reinforced concrete (RC) building by varying the transverse reinforcement spacing in both columns and beams. A six-story RC building was selected as the analytical model to investigate how different transverse reinforcement arrangements affect the structure's overall seismic response. The corresponding two-dimensional and three-dimensional representations of the building are presented in Figure 27. The structural layout was designed with uniform bay lengths of 5 m in both the X- and Y-directions.

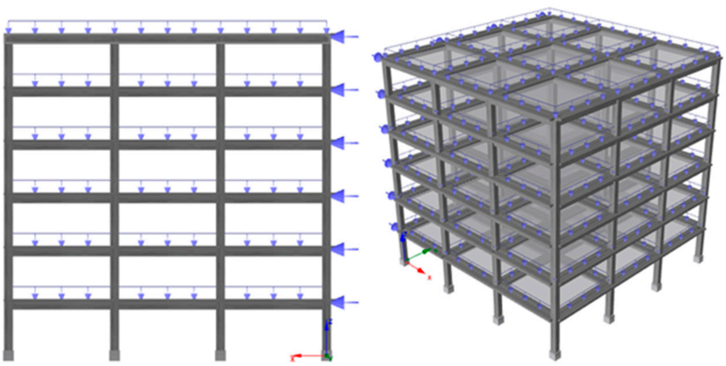

Figure 27. Two- and three-dimensional configurations of the reference RC structural model.

The formwork plan created for the structural model and the names of the columns are shown in Figure 28.

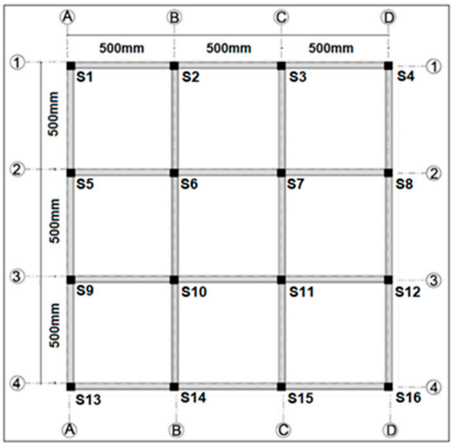

Figure 28. The blueprint of the story and display of columns.

Detailed specifications of the input parameters utilized in the numerical analysis are shown in Table 2.

Table 2. Constitutive parameters adopted for the numerical analysis.

Characteristic		Value
Concretes		C20/25
Reinforcements		S220
Beams (mm)		250 × 500 mm
Thickness of slabs (mm)		120 mm
Stories Height		3 m
Concrete Cover Thickness (mm)		25 mm
Columns		400 × 400 mm
	Corner	4Φ16
Longitudinal reinforcements (columns)	Top and bottom edge	4Φ16
	Right and left edges	4Φ16
Columns-Transverse reinforcements		Φ8/100-200-300-500
Beams-Transverse Reinforcements		Φ8/200
Local Soil class		ZA
Damping ratio		5%
Importance class		II
Target displacement (for six stories)		0.36 m

The same RC building model was considered in the structural analyses conducted for both columns and beams. The variables for each structural element were considered solely for that element, and results were obtained accordingly.

Across all structural models, both beams and columns were modeled using force-based plastic hinge frame elements (infrmFBPH). This formulation enables the spread of inelastic response over a prescribed portion of the member by means of force-based plasticity, thereby restricting nonlinear behavior to a finite hinge region. To ensure an accurate simulation of the stress–strain response, each cross-section was discretized into 100 fibers, which provides an adequate level of numerical precision for the adopted modeling approach. The plastic hinge length ratio (L_p/L) was assigned a value of 16.67%, consistent with established analytical methodologies and structural design recommendations. This ratio defines the portion of the member where plastic deformations are anticipated to localize during seismic excitation, promoting effective energy dissipation while maintaining the global stability of the structural system. The selected hinge length is in agreement with commonly accepted engineering practice for the representation of inelastic behavior in structural members. Furthermore, uniformly distributed loads were applied throughout all structural analyses.

The credibility and robustness of the numerical results are established through the use of well-calibrated and extensively validated modeling approaches implemented in the SeismoStruct platform. The force-based plastic hinge formulation combined with fiber-discretized cross-sections has been comprehensively verified in previous studies by comparison with independent experimental investigations involving both conventional and highly deficient RC columns. Furthermore, the constitutive material models employed in the present study, the Mander nonlinear concrete model for confined concrete and the Menegotto–Pinto steel model for reinforcing bars have demonstrated reliable performance in reproducing the behavior of substandard RC members subjected to monotonic and cyclic loading. Existing validation studies have confirmed that these material formulations can effectively capture the response of members characterized by poor concrete quality, insufficient transverse reinforcement, and smooth longitudinal reinforcement. The reported comparisons indicate that fiber-based distributed plasticity models accurately reproduce key structural response. Geometric nonlinearities were accounted for by enabling the P-Δ effect formulation across all structural nodes. The structural model was subjected to a displacement-controlled static pushover analysis using a uniform lateral load pattern applied at the story mass centers. The displacement of the roof center of mass was selected as the control node to monitor the target drift demands. The shear-failure criterion is defined in accordance with the shear capacity limit state specifications of EN 1998-3 (Eurocode 8). Throughout the nonlinear analysis, the algorithm continuously evaluates the evolving lateral shear demand against the dynamically calculated shear capacity of the structural members to identify the exact onset of failure.

4.1.1. Numerical Analysis Results for RC Columns

The fundamental objective of performance-based earthquake engineering is to evaluate the structural response under various predefined performance limit states. In this study, the performance criteria implemented in the SeismoStruct-2025 software were used to determine the demand and capacity limits associated with shear forces. To ensure consistency in the assessment, all columns were assigned identical transverse reinforcement spacing, allowing direct comparison of the resulting structural performance. A uniform transverse reinforcement spacing was adopted for all columns to facilitate the comparisons. The column cross-section and an example transverse reinforcement spacing considered in the study are shown in Figure 29.

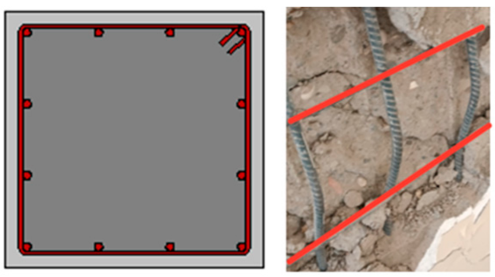

Figure 29. The column cross-section and an example transverse reinforcement spacing.

The numerical models were developed by varying the transverse reinforcement spacing. Five spacing values, namely 100, 200, 300, 400, and 500 mm, were analyzed to assess their influence on structural performance. The resulting demand and shear capacity values for the columns obtained from the analyses are summarized in Table 3. For all analytical models, transverse reinforcement with 135° hooks was adopted, while all remaining

https://doi.org/10.3390/buildings16142897

structural and material properties were maintained unchanged to ensure a consistent basis for comparison.

Table 3. Quantitative comparison between demand and capacity shear forces (kN).

Story	Column	Φ8/100 Model I Demand	Φ8/100 Model I Limit	Φ8/200 Model II Demand	Φ8/200 Model II Limit	Φ8/300 Model III Demand	Φ8/300 Model III Limit	Φ8/400 Model IV Demand	Φ8/400 Model IV Limit	Φ8/500 Model V Demand	Φ8/500 Model V Limit
1	S1			85.20	67.32	83.26	61.73	80.49	60.38	79.49	58.70
1	S2			95.03	79.47	94.28	73.57	92.56	71.78	91.42	69.85
1	S3			95.00	79.42	94.24	73.53	92.53	71.75	91.40	69.83
1	S4			85.18	67.31	83.25	61.72	80.48	60.36	79.49	58.69
1	S5			109.55	98.97	117.16	102.87	124.29	105.58	124.94	102.91
1	S6			111.07	104.28	119.23	103.05	131.21	108.78	133.57	108.87
1	S7			111.06	104.19	119.21	102.97	131.16	108.70	133.52	108.79
1	S8			109.55	98.99	117.16	102.88	124.29	105.60	124.95	102.93
1	S9			110.72	102.96	115.42	99.00	117.83	97.84	117.33	96.09
1	S10	No exceed		110.10	100.69	117.49	97.63	126.30	107.01	127.18	103.00
1	S11			110.13	100.79	117.52	97.72	126.34	107.10	127.22	103.06
1	S12			110.71	102.97	115.43	99.03	117.84	97.86	117.34	96.11
1	S13			110.70	100.47	118.24	99.55	126.25	105.51	126.59	102.51
1	S14			113.68	112.31	122.56	110.64	134.00	113.77	135.82	112.96
1	S15			113.68	112.30	122.55	110.63	133.99	113.76	135.82	112.96
1	S16			110.70	100.47	118.24	99.54	126.25	105.50	126.59	102.51
2	S1					No Exceed		66.31	65.15	66.95	62.46
2	S5			No Exceed		101.64	98.23	106.69	94.58	107.06	92.21
2	S9					102.32	99.19	105.05	92.81	104.46	89.53
2	S13					96.07	95.27	97.33	91.16	97.91	89.00

The structural deformation profiles and the corresponding failure modes under seismic loading for Model I through Model V are comparatively illustrated in Figure 30. In the red-colored columns, the shear force capacity has been exceeded, while in the gray-colored columns, there is no exceedance.

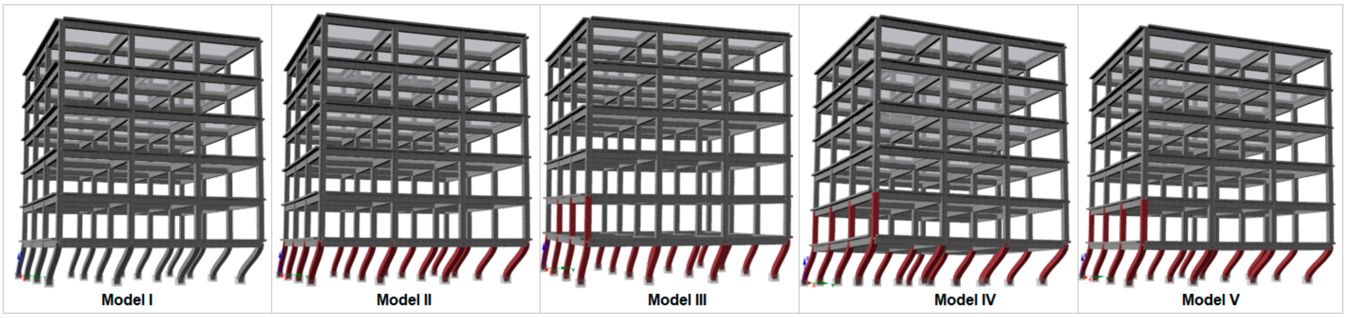

Figure 30. The shear force damage status for Model I—Model IV.

Based on the deformation analyses of Models I through V, it is concluded that structural irregularities significantly alter the seismic response and failure mechanisms of multi-story buildings. The localized stress concentrations observed in the lower-story columns emphasize the vital importance of structural uniformity. Consequently, the results demonstrate that strategic alterations in member stiffness can effectively control lateral drift and enhance overall structural resilience.

An increase in the spacing of transverse reinforcement in reinforced concrete (RC) columns results in a reduction in the available shear resistance provided by the confinement reinforcement. As a consequence, the probability of the applied shear demand exceeding the allowable shear capacity becomes significantly higher. The analytical results demonstrate that wider transverse reinforcement spacing leads to a greater number of columns surpassing their shear force capacity limits. When the spacing exceeds the maximum values prescribed by seismic design codes, longitudinal reinforcement becomes more susceptible to buckling, while the confined core concrete exhibits increasingly brittle behavior. Both the numerical analyses and post-earthquake field observations emphasize the necessity of complying with the transverse reinforcement detailing requirements specified in earthquake design regulations. Nevertheless, investigations of damaged structures have frequently revealed transverse reinforcement spacing considerably larger than the code-prescribed limits. In this stage of the study, transverse reinforcement spacing was treated as the sole variable, whereas all other structural parameters were kept unchanged. It should be noted, however, that additional factors, including concrete compressive strength, reinforcement properties, and reinforcement detailing, also have a significant influence on the failure mechanisms of RC columns. To further investigate the influence of transverse reinforcement detailing, additional analytical models were developed incorporating different stirrup diameters, 90° hook configurations, and conventional stirrup arrangements. The cross-sectional details of the columns, together with the characteristics of these analytical models, are summarized in Table 4.

Table 4. Details of the structural models developed for distinct column confinement scenarios.

Model	Cross-Section	Description
Model VI	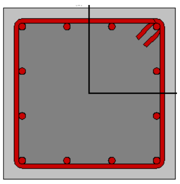	Transverse reinforcement Φ10/200
Model VII	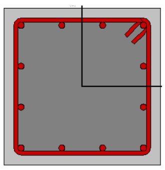	Transverse reinforcement Φ10/300
Model VIII	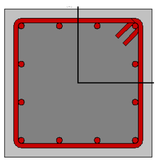	Transverse reinforcement Φ12/200
Model IX	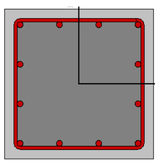	Transverse reinforcement 90° hooked; Φ8/200
Model X	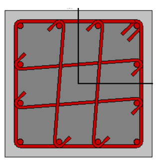	Reinforcement tie; Φ8/200

A comparative analysis of the shear forces across varying transverse reinforcement configurations is compiled in Table 5.

Table 5. Comparison of shear demand and shear capacity under different transverse reinforcement conditions.

<table>
<tr><th rowspan="2">Story</th><th rowspan="2">Column</th><th colspan="2">Model VI</th><th colspan="2">Model VII</th><th colspan="2">Model VIII</th><th colspan="2">Model IX</th><th colspan="2">Model X</th></tr>
<tr><th>Demand</th><th>Limit</th><th>Demand</th><th>Limit</th><th>Demand</th><th>Limit</th><th>Demand</th><th>Limit</th><th>Demand</th><th>Limit</th></tr>
<tr><td>1</td><td>S1</td><td colspan="2" rowspan="20">No exceed</td><td>86.55</td><td>79.16</td><td colspan="2" rowspan="20">No exceed</td><td>85.56</td><td>67.68</td><td colspan="2" rowspan="20">No exceed</td></tr>
<tr><td>1</td><td>S2</td><td>94.24</td><td>89.26</td><td>95.27</td><td>79.71</td></tr>
<tr><td>1</td><td>S3</td><td>94.21</td><td>89.23</td><td>95.23</td><td>79.66</td></tr>
<tr><td>1</td><td>S4</td><td>86.53</td><td>79.14</td><td>85.54</td><td>67.66</td></tr>
<tr><td>1</td><td>S5</td><td>98.32</td><td>98.03</td><td>108.18</td><td>98.31</td></tr>
<tr><td>1</td><td>S6</td><td colspan="2" rowspan="2">No Exceed</td><td>109.89</td><td>104.26</td></tr>
<tr><td>1</td><td>S7</td><td>109.88</td><td>104.18</td></tr>
<tr><td>1</td><td>S8</td><td>98.32</td><td>98.00</td><td>108.18</td><td>98.32</td></tr>
<tr><td>1</td><td>S9</td><td colspan="2" rowspan="2">No Exceed</td><td>109.39</td><td>102.35</td></tr>
<tr><td>1</td><td>S10</td><td>108.98</td><td>100.79</td></tr>
<tr><td>1</td><td>S11</td><td>118.06</td><td>117.88</td><td>109.01</td><td>100.89</td></tr>
<tr><td>1</td><td>S12</td><td colspan="2" rowspan="9">No Exceed</td><td>109.37</td><td>102.34</td></tr>
<tr><td>1</td><td>S13</td><td>109.61</td><td>100.42</td></tr>
<tr><td>1</td><td>S14</td><td>112.15</td><td>112.00</td></tr>
<tr><td>1</td><td>S15</td><td>112.15</td><td>111.99</td></tr>
<tr><td>1</td><td>S16</td><td>109.61</td><td>100.43</td></tr>
<tr><td>2</td><td>S1</td><td colspan="2" rowspan="4">No exceed</td></tr>
<tr><td>2</td><td>S5</td></tr>
<tr><td>2</td><td>S9</td></tr>
<tr><td>2</td><td>S13</td></tr>
</table>

The distribution of shear failure locations across the vertical elements for Models VI to X is systematically presented in Figure 31.

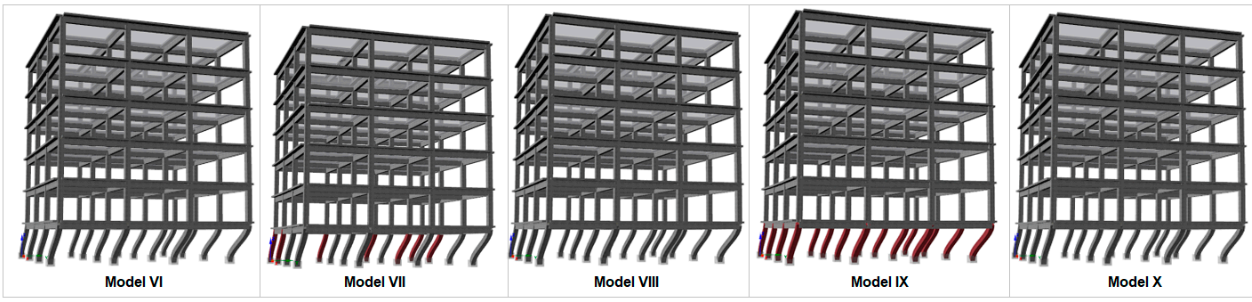

Figure 31. Comparative evaluation of the localized shear failure mechanisms for Models VI through X under seismic demand.

Based on the comparative analysis of Models VI to X, it is concluded that structural modifications play a critical role in mitigating or exacerbating shear concentration risks during seismic events. The localized damage patterns restricted primarily to the ground floor underscore the high susceptibility of the lower stories to lateral displacement demands. Therefore, the findings suggest that implementing uniform structural stiffness and adequate shear retrofitting at the base level are vital strategies for ensuring structural stability.

Current Turkish seismic design regulations require the use of special seismic stirrups in reinforced concrete members. The findings of the structural analyses strongly support the effectiveness of this requirement. In Model X, where additional stirrups were incorporated, none of the columns exceeded their allowable shear limits. The increase in transverse reinforcement per unit cross-sectional area enhanced the shear capacity of the columns, resulting in improved structural performance. Furthermore, enlarging the diameter of the transverse reinforcement provided an additional increase in shear resistance.

Accordingly, Models VI and VIII exhibited no columns exceeding the prescribed shear capacity, with higher transverse reinforcement diameters contributing to greater shear strength. In contrast, Model VII, characterized by excessive stirrup spacing, showed seven columns exceeding the allowable shear force, demonstrating that reinforcement spacing remains a critical parameter governing column performance. The Turkish Earthquake Code also specifies that transverse reinforcement should be anchored using 135° hooks to ensure adequate confinement and reliable anchorage of the longitudinal reinforcement during seismic loading. This detailing allows the transverse reinforcement to effectively restrain the longitudinal bars and maintain their structural function under earthquake-induced deformations. Nevertheless, post-earthquake field investigations have frequently identified damaged columns containing stirrups with 90° hooks instead of the required 135° configurations. To evaluate the consequences of this detailing deficiency, Model IX was developed using 90° hook anchorage. The analysis indicated that 16 columns exceeded their allowable shear capacities, confirming the detrimental effect of inadequate anchorage on seismic performance. A summary of the number of columns exceeding the prescribed limit state for each analytical model is presented in Table 6.

Table 6. Columns exceeding the ehear resistance limit.

Model	Total Number of Columns	Number of Columns Exceeding the Limit	%
I	96	0	0
II	96	16	17
III	96	19	20
IV	96	20	21
V	96	20	21
VI	96	0	0
VII	96	7	7
VIII	96	0	0
IX	96	16	17
X	96	0	0

The quantitative damage distribution assessment across Models I to X indicates that structural modifications drastically alter the severe stress concentrations in the vertical structural components. While specific configurations such as Models I, VI, VIII, and X completely avoided capacity exceedance, Models IV and V exhibited the highest vulnerability, with 21% of their columns exceeding design thresholds. These results conclude that optimizing structural uniformity is a critical prerequisite to mitigating structural column failures during major seismic events.

4.1.2. Numerical Analysis Results for RC Beams

The properties of the models created using different variables for RC beams are given in Table 7.

Table 7. Beam models with different stirrup configurations.

Model	Description
XI	Transverse reinforcement Φ8/200
XII	Transverse reinforcement Φ8/400
XIII	Transverse reinforcement Φ8/500
XIV	Transverse reinforcement Φ10/200
XV	Transverse reinforcement 90° hooked; Φ8/200

The number of beams where the shear force limit values are exceeded for the models considered as a result of structural analyses is shown in Table 8.

Table 8. Number of beams exceeding the shear force limit.

Model	Total Number of Beams	Number of Exceeding Beams	%
XI	144	4	3
XII	144	14	10
XIII	144	20	14
XIV	144	0	0
XV	144	4	3

The spatial distribution of shear-induced damage across the lower floor levels for Models XI to XV is comparatively illustrated in Figure 32.

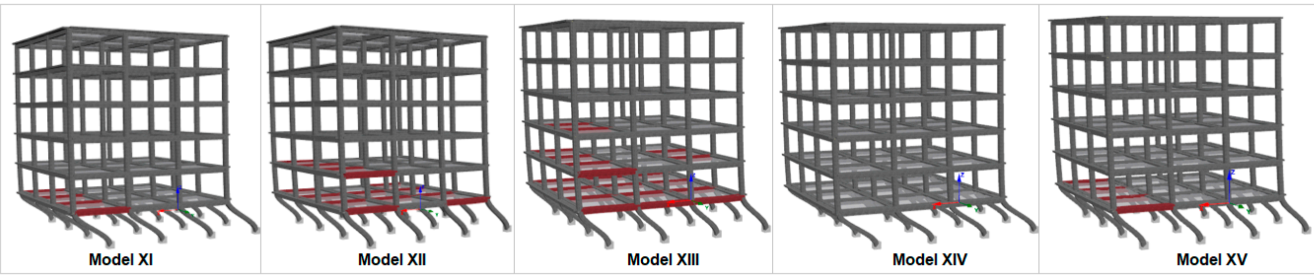

Figure 32. Comparative visualization of the seismic deformation configurations and beam shear damage patterns for Models XI through XV.

Based on the comparative performance of Models XI to XV, it is concluded that structural modifications extensively redistribute the lateral shear demands across the lower stories. The prominent damage observed within the lower floor systems highlights the critical role of diaphragm stiffness in governing global seismic behavior. Consequently, the findings emphasize that strengthening both the base columns and the associated horizontal frame connections is essential to achieve balanced energy dissipation and prevent localized brittle failure.

4.1.3. Analysis Results for Other Structural Models

Different variables for beams and columns have been implemented specifically for these elements. Observational field studies revealed that in some columns and beams, the transverse reinforcement was plain while the longitudinal reinforcement was ribbed. In this context, Model XVI was created considering the material differences of both longitudinal and transverse reinforcement in beams and columns. To facilitate comparison, Model XVII was created where both transverse and longitudinal reinforcements belong to the same type of reinforcement class. In Model XVIII, where the concrete properties supporting the shear force with transverse reinforcement are weak, the concrete class was considered as C8/10. Model XIX takes into account the use of diamond stirrups in RC columns. The created models and their details are presented in Table 9.

To rigorously isolate the individual structural effects of steel grade, concrete strength, and transverse tie configuration without confounding variables, the parametric analysis for Models XVI through XIX was evaluated using strictly controlled, single-variable comparative subsets. Within this analytical framework, the impact of each mechanical property is quantified by altering only one targeted parameter at a time while maintaining all other material strengths and detailing configurations completely constant. This systematic approach ensures that the independent sensitivity of steel grade, concrete grade, and tie spacing on the ultimate shear capacity and displacement performance is transparently isolated, preventing any overlapping or compounding analytical effects.

Table 9. Structural models developed for different parameters.

Model	Summary
Model XVI	Transverse and Longitudinal reinforcement S220
Model XVII	Transverse and longitudinal reinforcement S420
Model XVIII	Transverse/longitudinal reinforcement S220; Concrete grade C8/10
Model XIX	Diamond reinforcement ties in columns

The total count of structural elements exceeding their threshold shear limits is tabulated in Table 10 for each model scenario.

Table 10. Number of elements where limit shear forces are exceeded for different structural models.

Model	Columns			Beams		
	Total Number of Columns	Number of Exceeding Columns	%	Total Number of Beams	Number of Exceeding Beams	%
Model XVI	96	20	21	144	8	6
Model XVII	96	4	4	144	0	0
Model XVIII	96	20	21	144	36	25
Model XIX	96	0	0	144	0	0

Based on the results presented in Table 10, Model XIX achieved the most favorable performance, with no columns or beams exceeding the specified performance limit, indicating the effectiveness of the adopted reinforcement strategy. In contrast, Model XVIII exhibited the highest proportion of deficient members, with 21% of the columns and 25% of the beams exceeding the limit state, reflecting the least satisfactory structural response among the investigated models. Model XVII also demonstrated a significant improvement compared to Model XVI, reducing the percentage of exceeding columns from 21% to 4% while completely eliminating beam deficiencies.

The structural responses and localized shear damage patterns within the lower-story frames for Models XVI to XIX are comparatively demonstrated in Figure 33.

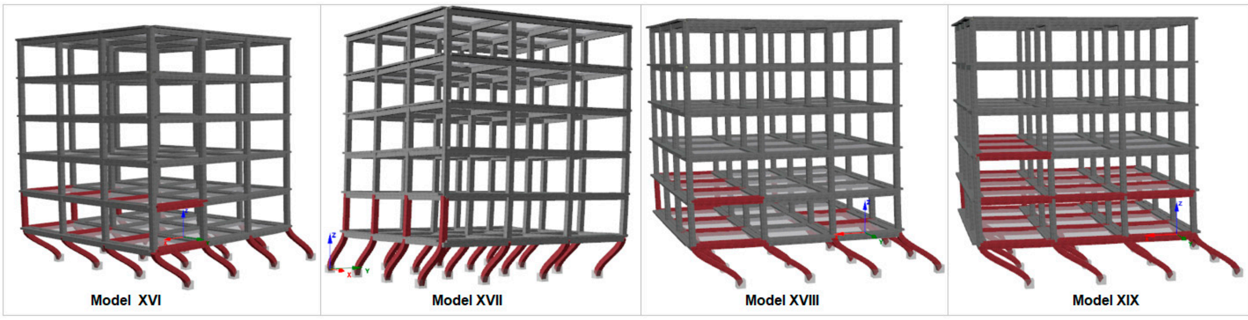

Figure 33. Comparative illustration of the column failures and corresponding structural member damage distributions for Models XVI through XIX under seismic action.

Based on the deformation characteristics observed from Models XVI to XIX, it is concluded that structural modifications significantly alter the shear demand path across the lower stories. The simultaneous yielding of the ground columns and the adjacent floor beams highlights the high demand for energy dissipation in these critical zones. Consequently, the results demonstrate that strategic reinforcement of both frame connections and vertical load-bearing elements is essential to secure overall structural integrity.

4.2. Element-Based Numerical Analysis

The element-based shear forces for the columns in this structural model were also obtained according to Eurocode-8. The element-based shear force capacities obtained for each model are shown in Table 11.

Table 11. The element-based shear forces for the columns.

Model	Shear Force Capacity (kN)
I	122.71
II	96.11
III	87.25
IV	82.82
V	80.16
VI	110.26
VII	96.56
VIII	127.21
IX	96.11
X	122.71

Within the scope of the study, beams were selected as 250 × 500 mm. Element-based shear force capacities of the models selected according to Eurocode-8 are shown in Table 12.

Table 12. The element-based shear forces for the beams.

Model	Shear Force Capacity (kN)
XI	63.29
XII	45.65
XIII	42.12
XIV	82.50
XV	63.29

Element-based shear force capacities in structural models where the transverse reinforcement conditions in columns and beams change together are shown in Table 13.

Table 13. The element-based shear forces for the columns and beams.

Model	Columns Ultimate Shear Capacity (kN)	Beams Ultimate Shear Capacity (kN)
XVI	96.11	82.50
XVII	120.29	95.37
XVIII	75.09	53.00
XIX	122.71	63.29

4.3. Comparison of Target Displacements

Performance-based earthquake engineering mainly focuses on target displacement as an important outcome [87,88]. The target displacements have been determined based on the limit states outlined in Eurocode 8, which is more widely used globally. These limit states are presented in Table 14.

The target displacement demands derived for all numerical models under varying column design variables are summarized in Table 15.

With increasing spacing of the transverse reinforcement, the target displacements have decreased to ensure structural safety. The lowest target displacements were achieved with transverse reinforcements bent at a 90° angle. In the models created considering other transverse reinforcement conditions, there is no significant change in the target displacements. When different conditions of transverse reinforcement are considered for beams, it has been found that the target displacements exhibit very minor differences. This once again emphasizes the necessity for a stronger design of columns compared to beams. While beams are only related to the loads on their respective floors, columns are connected to other columns on different stories.

Table 14. Performance Levels Defined by Eurocode 8 (Part 3) [89,90].

Limit State	Description	Return Period (Year)	Probability of Exceedance (in 50 Years)
Limit state of damage limitation (DL)	Only lightly damaged, damage to non-structural components economically repairable.	225	0.20
Limit state of significant damage (SD)	Significantly damaged, some residual strength and stiffness, non-structural components damaged, uneconomic to repair.	475	0.10
Limit state of near collapse (NC)	Heavily damaged, very low residual strength and stiffness, large permanent drift but still standing.	2475	0.02

Table 15. Summary of target displacements.

Model	Target Displacements (m)		
	DL	SD	NC
Model I	0.06138476	0.07874644	0.13651848
Model II	0.06135176	0.0787041	0.13644509
Model III	0.06134131	0.07869069	0.13642184
Model IV	0.06133584	0.07868368	0.13640968
Model V	0.04687658	0.06013485	0.10425258
Model VI	0.06143582	0.07881195	0.13663205
Model VII	0.06140414	0.0787713	0.13656159
Model VIII	0.0615396	0.07894508	0.13686285
Model IX	0.04687658	0.06013485	0.10425258
Model X	0.06138779	0.07875033	0.13652522
Model XI	0.061388	0.07875	0.136525
Model XII	0.061385	0.078747	0.136519
Model XIII	0.061385	0.078747	0.136519
Model XIV	0.061445	0.078823	0.136651
Model XV	0.061385	0.078747	0.136519
Model XVI	0.066076	0.084765	0.146952
Model XVII	0.066217	0.084945	0.147265
Model XVIII	0.070348	0.090245	0.156452
Model XIX	0.061406	0.078773	0.136565

The parametric sensitivity analysis conducted across twenty distinct structural configurations of a typical six-story reinforced concrete (RC) building framework yielded critical quantitative insights into the structural implications of transverse reinforcement detailing. Notably, the numerical simulations demonstrate that optimizing the stirrup spacing by reducing it from 300 mm to 200 mm enhances the column shear capacity by up to 10%, thereby significantly mitigating the risk of brittle fracture. Conversely, detailing deficiencies such as excessive spacing directly exacerbate vulnerability; for instance, Model VII, characterized by such excessive spacing, resulted in seven columns exceeding their allowable shear force capacity. Furthermore, the detrimental compounding effect of material sub-standardization is highlighted by the fact that low-strength concrete (C8/10) induces up to a 40% reduction in shear capacity compared to the reference C20/25 concrete grade under identical reinforcement setups. In contrast, the implementation of contemporary seismic provisions specifically through the integration of special seismic crossties in Model X completely eliminated shear capacity exceedances across all vertical members. These quantitative findings emphasize that while reinforcement detailing parameters such as spacing, rebar diameter, and a mandatory 135° hook angle dictate the threshold of crack initiation and longitudinal bar buckling, proper on-site execution and material strength remain paramount to preventing catastrophic global failure.

The target displacement of 0.36 m represents the theoretical seismic deformation demand imposed on the building by the design earthquake, evaluated in accordance with the Eurocode 8 N2 method. In contrast, the values of 0.104–0.157 m denote the actual lateral displacement capacity of the deficient models at the Near-Collapse performance level. Since the required seismic demand vastly exceeds the available structural capacity, these findings mathematically justify the severe damage and collapse mechanisms documented during our field investigations.

4.4. Strengthening Solution

In this part of the study, reinforcement with steel fibers was planned for Model II, which has a shear force effect. 16 columns, whose shear force capacity was exceeded, were reinforced using steel fibers, and structural analyses were performed. Steel and similar fibers are among the modern reinforcement materials preferred today for increasing shear force capacity. In recent years, fiber-reinforced materials have gained increasing attention in structural engineering as effective strengthening solutions for reinforced concrete members. Among these materials, steel fibers and other similar fiber-based reinforcement systems are widely adopted modern techniques aimed at enhancing the shear capacity and overall structural performance of structural elements. These materials are particularly valued for their ability to improve load transfer mechanisms, delay crack propagation, and enhance post-cracking behavior. As a result, the incorporation of fiber reinforcement has become an important approach in both new construction and strengthening applications, especially in improving the shear resistance of structural components under critical loading conditions. Typical properties of the steel fiber considered in this paper are given in Table 16.

Table 16. Typical properties of the steel fiber.

Characteristic	Value
Fibre’s Thickness (mm)	0.3810
Strength in Tension (MPa)	3400
Modulus of elasticity (MPa)	190,000
Ultimate Elongation (%)	2.30
Areal Weight (g/m^2)	3300

The RC column cross-sections before and after reinforcement are illustrated in Figure 34.

To systematically restore the shear capacity of the deficient RC columns, FRP retrofitting scheme was designed and numerically simulated. The composite material utilized consists of high-strength unidirectional FRP sheets characterized by a nominal design thickness of 0.3810 mm, a tensile strength of 3400 MPa, and an elastic modulus of 190 GPa. The retrofitting configuration employs a single-layer, fully wrapped continuous jacket with the carbon fibers oriented horizontally (perpendicular to the longitudinal axis of the columns) to specifically resist lateral shear demands and enhance concrete confinement. To ensure a realistic performance limit and prevent premature brittle failures, the design limits the effective strain of the FRP wrap well below its ultimate rupture strain, explicitly accounting for debonding checks. This effective strain limit was calculated based on the substrate concrete strength and the confinement configuration, in strict accordance with the retrofitting guidelines of international seismic codes, thereby ensuring that the documented capacity enhancements are both structurally reliable and physically achievable.

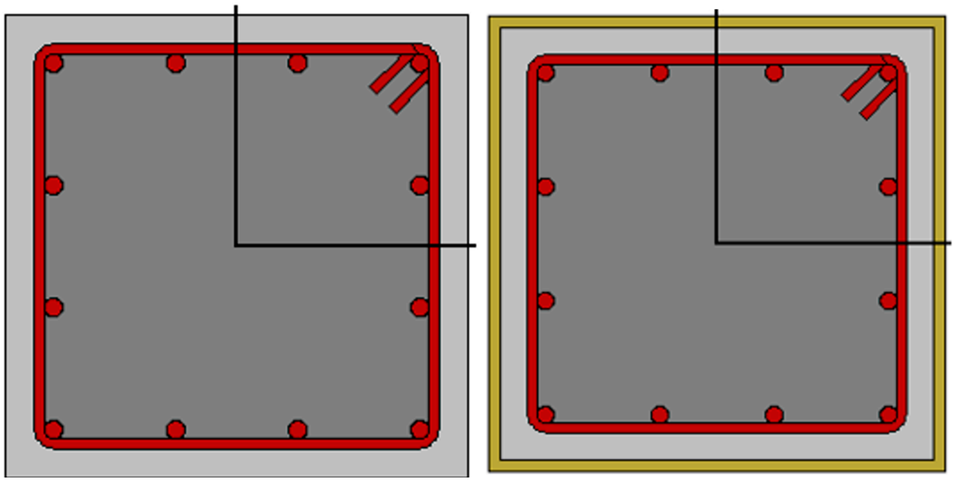

Figure 34. Cross-Sections of RC Columns before and after Strengthening.

In the reference analytical model, the columns identified as exceeding their shear capacity were retrofitted using a steel fiber reinforcement system. The strengthening intervention was applied to all first-story columns. During the retrofit process, the steel fiber was assumed to be installed continuously over the full height of each column without interruptions. In the numerical analyses, the fiber-reinforced polymer (FRP) material was modeled as a single continuous layer. To account for proper fiber application, the corners of the column sections were assumed to be rounded with a radius of 40 mm. A comparison of the shear damage conditions before and after the strengthening intervention is presented in Figure 35.

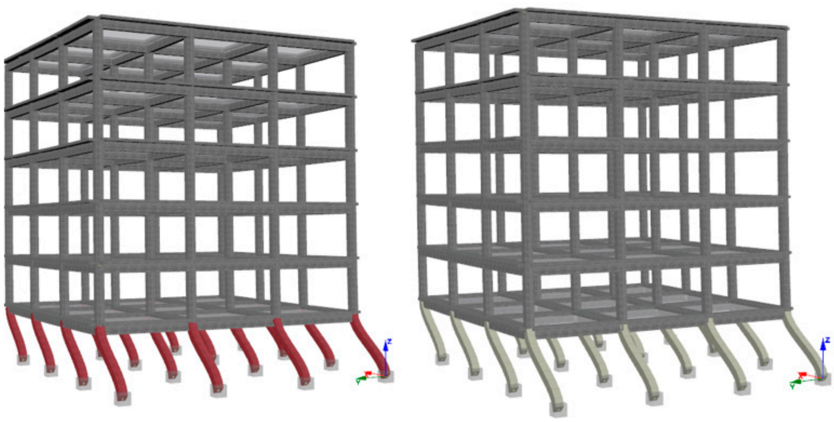

Figure 35. The shear force damage status before and after reinforcement.

There was no exceedance in the shear force capacities of the columns strengthened with steel fiber on the ground floor. This once again demonstrates the usability of steel fibers and similar fibers in increasing the shear force capacity of structural elements.

The sequential implementation phases of the FRP wrapping application, spanning from initial substrate preparation to the final protective topcoat installation, are systematically illustrated in Figure 36.

Figure 36. Schematic step-by-step procedure for the seismic retrofitting of a reinforced concrete column using FRP wrapping.

To ensure the full composite action and efficiency of the retrofitting scheme, strict adherence to quality control measures during each application stage is imperative. Particular attention must be paid to achieving a completely dust-free substrate during surface preparation and ensuring full impregnation of the carbon fiber sheet without trapped air bubbles during resin application. Furthermore, the application of a UV-resistant protective topcoat is vital to prevent long-term environmental degradation of the epoxy matrix, thereby maintaining the structural integrity of the retrofitted element.

5. Conclusions

In Türkiye, which has experienced significant earthquakes, two earthquakes occurred on 6 February 2023, close to the same province, causing extensive damage and destruction to structural systems. The irregularities in the urban building stock, particularly in RC structures, and the structural characteristics that do not comply with earthquake regulations exacerbated the extent of the devastation. This study focuses on the conditions of transverse reinforcement in columns and beams, particularly concerning resisting shear forces.

Transverse reinforcement, especially in the context of earthquake effects, enhances the strength and ductility of structural elements. The spacing in areas of confinement should be carefully considered, and hooks should be bent at a 135° angle toward the inside of the concrete to ensure proper anchoring to the longitudinal reinforcement.

The analytical results show that increasing the spacing of transverse reinforcement and reducing its diameter increase the likelihood of shear failure in RC columns and beams. Comprehensive structural analyses were performed to evaluate the influence of different transverse reinforcement parameters. The findings confirm the importance of proper reinforcement detailing and good construction practice for satisfactory seismic performance. The principal findings are summarized as follows:

- An increase of up to 10% in shear capacity is achieved by reducing the transverse reinforcement spacing from 300 mm to 200 mm
- A 15% to 18% enhancement in shear capacity is realized when the bar diameter is increased from Φ8 to Φ12.
- Utilizing a 135° hook anchorage provides superior confinement, thereby significantly suppressing the lateral buckling of longitudinal bars
- FRP retrofitting restored capacity in all deficient columns tested.
- A structural capacity loss of up to 40% is observed when low-strength concrete is paired with deficient reinforcement configurations.

In the Turkish Earthquake Regulations, the spacing of stirrups is limited differently for columns and beams. The spacing of transverse reinforcement must not exceed the limit states specified in the regulations. To prevent any disruption in the position and arrangement of transverse reinforcement, it is important to ensure proper anchoring during the application phase, and special care should be taken with the use of crossties in columns.

Field observations also showed that reinforcement corrosion and the use of plain reinforcement significantly reduced the seismic performance of RC members. Corrosion decreased the reinforcement cross-section and weakened the bond between concrete and steel, while plain reinforcement increased the risk of bond failure because of its poor mechanical interlock. These problems became more critical in older buildings with low-strength concrete and inadequate construction practices.

Based on the findings obtained from both post-earthquake field investigations and the structural analyses, the principal factors influencing the effectiveness and intended performance of transverse reinforcement can be summarized as follows:

- Diameter of the transverse reinforcement;
- Spacing between transverse reinforcement elements;
- Combined use of different reinforcement types within the same structural member;
- Use of plain reinforcing bars instead of deformed reinforcement;
- Low concrete compressive strength;
- Reinforcement corrosion;
- Absence of supplementary cross-ties (stirrups) in columns;
- Inadequate hook angle of the transverse reinforcement;
- Deficient reinforcement detailing and construction workmanship;
- Insufficient concrete cover thickness;
- Inadequate anchorage between transverse and longitudinal reinforcement.

A parametric sensitivity analysis was performed to quantify the relative influence of each transverse reinforcement variable on shear force capacity. Results indicate that reinforcement spacing has the highest impact, followed by hook angle, diameter, and steel grade. Concrete strength significantly modulates these effects, with low-strength concrete (C8/10) showing up to 40% reduction in capacity compared to C20/25 for identical reinforcement configurations. The numerical findings align with observed field damage patterns, confirming that transverse reinforcement deficiencies directly reduce shear capacity and ductility in both columns and beams. Comparisons with TBEC-2018 show that while current codes prescribe adequate spacing and anchorage requirements, field execution often falls short, particularly in older pre-2000 structures. Introducing stricter inspection protocols and on-site verification during construction could mitigate these deficiencies.

Although pushover analysis effectively quantifies shear force exceedance and structural deformation profiles under simulated lateral drift, it may not fully capture the complex, cyclic degradation and high-frequency dynamic effects induced by consecutive seismic shocks, such as the 2023 Kahramanmaraş twin earthquakes. The adopted approach also does not fully consider higher-mode effects and torsional behavior. In addition, different ground motion characteristics may lead to different structural responses. Therefore, the results should be considered within the scope of the selected analysis method. Nonetheless, the accuracy of the numerical findings is validated by their strong correlation with the qualitative field damage patterns.

The combined field observations and numerical analyses provide practical recommendations for the seismic assessment and strengthening of existing RC buildings. Comparisons with TBEC-2018 show that the code requirements for transverse reinforcement are generally adequate. However, many of the observed failures were related to poor detailing and construction workmanship. The results indicate that reducing stirrup spacing to

200 mm and using 135° hooks improve the shear performance of RC members. In addition, FRP strengthening was found to be an effective method for restoring the shear capacity of deficient columns.

Future studies may include nonlinear time-history analyses to better evaluate the seismic response under different earthquake records. Experimental studies on reinforcement corrosion and bond deterioration may also improve the understanding of long-term structural performance. In addition, different strengthening materials and retrofit techniques can be investigated and compared.

Author Contributions: Conceptualization, E.I., F.A. and D.R.; methodology, E.I., E.H., A.B. and F.A.; validation, M.H.-N. and E.A.; investigation, E.I. and F.A.; resources, A.B. and D.R.; data curation, E.H., E.A. and M.H.-N.; writing—original draft preparation, E.I., D.R. and A.B.; writing—review and editing, F.A., E.A., E.H. and M.H.-N.; visualization, E.I. and E.A.; supervision, A.B. and M.H.-N.; funding acquisition, E.H. All authors have read and agreed to the published version of the manuscript.

Funding: No external funding was received for this research.

Data Availability Statement: All data supporting the findings of this study are included in this article.

Acknowledgments: The results presented in this scientific paper were partially obtained through research activities within the project 2023-1-HR01-KA220HED-000165929 "Intelligent Methods for Structures, Elements, and Materials" (https://im4stem.eu/en/home/, accessed on 12 October 2025) under the Erasmus+ KA220-HED Cooperation Partnerships in Higher Education program of the European Union.

Conflicts of Interest: The authors have no conflicts of interest to declare.

References

1. Valente, M. Seismic Upgrading Strategies for Non-Ductile Plan-Wise Irregular R/C Structures. *Procedia Eng.* **2013**, *54*, 539–553. [CrossRef]
2. Ruggieri, S.; Uva, G. Accounting for the Spatial Variability of Seismic Motion in the Pushover Analysis of Regular and Irregular RC Buildings in the New Italian Building Code. *Buildings* **2020**, *10*, 177. [CrossRef]
3. Chaulagain, H.; Rodrigues, H.; Jara, J.; Spacone, E.; Varum, H. Seismic Response of Current RC Buildings in Nepal: A Comparative Analysis of Different Design/Construction. *Eng. Struct.* **2013**, *49*, 284–294. [CrossRef]
4. Valente, M. Seismic Rehabilitation of a Three-Storey R/C Flat-Slab Prototype Structure Using Different Techniques. *Appl. Mech. Mater.* **2012**, *193*, 1346–1351.
5. Ruggieri, S.; Chatzidaki, A.; Vamvatsikos, D.; Uva, G. Reduced-Order Models for the Seismic Assessment of Plan-Irregular Low-Rise Frame Buildings. *Earthq. Eng. Struct. Dyn.* **2022**, *51*, 3327–3346.
6. De Luca, F.; Woods, G.E.; Galasso, C.; D'Ayala, D. RC Infilled Building Performance against the Evidence of the 2016 EEFIT Central Italy Post-Earthquake Reconnaissance Mission: Empirical Fragilities and Comparison with the FAST Method. *Bull. Earthq. Eng.* **2018**, *16*, 2943–2969.
7. Valente, M. Seismic Strengthening of Non-Ductile R/C Structures Using Infill Wall or Ductile Steel Bracing. *Adv. Mater. Res.* **2012**, *602–604*, 1583–1587. [CrossRef]
8. Bianchi, F.; Nascimbene, R.; Pavese, A. Experimental vs. Numerical Simulations: Seismic Response of a Half Scale Three-Storey Infilled RC Building Strengthened Using FRP Retrofit. *Open Civ. Eng. J.* **2017**, *11*, 1158–1169. [CrossRef]
9. Pohoryles, D.A.; Melo, J.; Rossetto, T.; Varum, H.; D'Ayala, D. Effect of Slab and Transverse Beam on the FRP Retrofit Effectiveness for Existing Reinforced Concrete Structures under Seismic Loading. *Eng. Struct.* **2021**, *234*, 111991. [CrossRef]
10. Nascimbene, R.; Bellotti, D.; Bianchi, F.; Brunesi, E. Numerical Seismic Performance of a Beam–Column Connection in Hospital RC Buildings Retrofitted with Dissipative Bracing: Implications for Behaviour Factor Evaluation. *Appl. Sci.* **2026**, *16*, 4861. [CrossRef]
11. Avcil, F.; Peker, F.Ü.; Harrat, Z.R.; Işık, E.; Hadzima-Nyarko, M. Effectiveness of FRP Strengthening on RC Columns with Multiple Structural Deficiencies: A Numerical Investigation. *Buildings* **2026**, *16*, 2372. [CrossRef]
12. Pirmoradi, P.; Suiker, A.S.; Poorsolhjouy, P. Multi-scale constitutive model for fiber-reinforced concrete with FEM analyses of structural failure. *Eng. Fract. Mech.* **2025**, *323*, 111166. [CrossRef]
13. Karasin, I.B. Analytic investigation of hooked stirrups on seismic behavior of reinforced concrete 3D frame buildings. *Appl. Sci.* **2023**, *13*, 11590. [CrossRef]

14. Ren, D.; Wang, Z.; Kong, L.; Wu, P.; Sun, J.; Dai, G.; Ai, C. Full-time domain rust expansion investigation and visual evaluation of reinforced concrete under synergistic protection. *Eng. Fract. Mech.* **2025**, *314*, 110677. [CrossRef]
15. Suárez, F.; Donaire-Ávila, J.; Aceituno, J.F. An automatic procedure for calibrating the fracture parameters of fibre-reinforced concrete. *Eng. Fract. Mech.* **2025**, *318*, 110919. [CrossRef]
16. Nitka, M.; Tejchman, J. Mesoscopic simulations of a fracture process in reinforced concrete beam in bending using a 2D coupled DEM/micro-CT approach. *Eng. Fract. Mech.* **2024**, *304*, 110153. [CrossRef]
17. Işık, E.; Shao, Y.B.; Hadzima-Nyarko, M.; Radu, D.; Bulajic, B.; Lozancic, S. Enhancing the Seismic Safety of Upgraded RC Buildings Using FRP Retrofitting: Analytical and Field Evidence from the 2023 Kahramanmaraş Earthquakes. *Bull. Earthq. Eng.* **2026**, *24*, 1467–1501.
18. Xue, L.; Ren, X.; Ballarini, R. Damage-plasticity modeling of shear failure in reinforced concrete structures. *Eng. Fract. Mech.* **2023**, *290*, 109536. [CrossRef]
19. Accornero, F.; Rubino, A.; Carpinteri, A. A fracture mechanics approach to the design of hybrid-reinforced concrete beams. *Eng. Fract. Mech.* **2022**, *275*, 108821. [CrossRef]
20. Kurumatani, M.; Soma, Y.; Terada, K. Simulations of cohesive fracture behavior of reinforced concrete by a fracture-mechanics-based damage model. *Eng. Fract. Mech.* **2019**, *206*, 392–407. [CrossRef]
21. Yuan, C.; Chen, W.; Pham, T.M.; Hao, H.; Cui, J.; Shi, Y. Influence of concrete strength on dynamic interfacial fracture behaviour between fibre reinforced polymer sheets and concrete. *Eng. Fract. Mech.* **2020**, *229*, 106934. [CrossRef]
22. İnce, E.G.; Çakıl, B.; Şimşek, M.; İnce, O. Evaluation of Ground Motions and Seismic Performance of RC Buildings after 2023 Kahramanmaraş Earthquakes: Design and Construction Deficiencies. *Bull. Earthq. Eng.* **2026**, *24*, 727–754.
23. Eken, M. Post-Earthquake Field Assessment and Damage Correlation of Elevated Reinforced Concrete Water Tanks in Kahramanmaraş/Elbistan, Türkiye. *Struct. Concr.* **2026**. [CrossRef]
24. Tonyali, Z.; Kiral, A.; Ergun, M.; Garcia, R. Seismic Resilience of Existing RC Dual-System Buildings during the 2023 Kahramanmaraş Earthquakes: A Case Study. *J. Asian Archit. Build. Eng.* **2026**, 1–26. [CrossRef]
25. Yadim, Y.; Yılmaz, S.; Kaplan, H.; Corradi, M.; Castori, G. Seismic Vulnerability of Deficient RC Buildings: Insights from the February 6, 2023, Turkey Earthquake. *Procedia Struct. Integr.* **2026**, *78*, 1895–1902. [CrossRef]
26. Işık, E.; Avcil, F.; Büyüksaraç, A.; Arkan, E.; Lozančić, S.; Radu, D.; Hadzima-Nyarko, M. Influence of Transverse Reinforcement on Damage and Fracture Mechanisms in RC Structures during the Kahramanmaraş Earthquakes. *Procedia Struct. Integr.* **2026**, *77*, 465–474. [CrossRef]
27. Atasever, K.; Aydogdu, H.H.; Narlitepe, F.; Goksu, C.; Demir, U.; Demir, C.; Ilki, A. Damage Assessment of Structures Following the February 6, 2023 Kahramanmaraş Earthquakes: A Dataset-Based Case Study in Gaziantep, Türkiye. *Arab. J. Sci. Eng.* **2026**, *51*, 693–715.
28. Sezen, H.; Whittaker, A.S.; Elwood, K.J.; Mosalam, K.M. Performance of reinforced concrete buildings during the August 17, 1999 Kocaeli, Turkey earthquake, and seismic design and construction practise in Turkey. *Eng. Struct.* **2003**, *25*, 103–114. [CrossRef]
29. Kaplan, H.; Yilmaz, S.; Binici, H.; Yazar, E.; Çetinkaya, N. May 1, 2003 Turkey-Bingöl earthquake: Damage in reinforced concrete structures. *Eng. Fail. Anal.* **2004**, *11*, 279–291. [CrossRef]
30. Doğangün, A. Performance of reinforced concrete buildings during the May 1, 2003, Bingöl Earthquake in Turkey. *Eng. Struct.* **2004**, *26*, 841–856. [CrossRef]
31. Arslan, M.H.; Korkmaz, H.H. What is to be learned from damage and failure of reinforced concrete structures during recent earthquakes in Turkey? *Eng. Fail. Anal.* **2007**, *14*, 1–22. [CrossRef]
32. Inel, M.; Ozmen, H.B.; Bilgin, H. Re-evaluation of building damage during recent earthquakes in Turkey. *Eng. Struct.* **2008**, *30*, 412–427. [CrossRef]
33. İlki, A.; Celep, Z. Earthquakes, existing buildings and seismic design codes in Turkey. *Arab. J. Sci. Eng.* **2012**, *37*, 365–380. [CrossRef]
34. Tapan, M.; Comert, M.; Demir, C.; Sayan, Y.; Orakcal, K.; Ilki, A. Failures of structures during the October 23, 2011, Tabanlı (Van) and November 9, 2011 Edremit (Van) earthquakes in Turkey. *Eng. Fail. Anal.* **2013**, *34*, 606–628. [CrossRef]
35. Inel, M.; Ozmen, H.B.; Akyol, E. Observations on the building damages after 19 May 2011 Simav (Turkey) earthquake. *Bull. Earthq. Eng.* **2013**, *11*, 255–283.
36. Çelebi, E.; Aktas, M.; Çağlar, N.; Özocak, A.; Kutanis, M.; Mert, N.; Özcan, Z. October 23, 2011 Turkey/Van-Ercis earthquake: Structural damages in the residential buildings. *Nat. Hazards* **2013**, *65*, 2287–2310.
37. Hadzima-Nyarko, M.; Işık, E.; Radu, D.; Bulajić, B.; Lozančić, S.; Radić, J.; Ereš, A. Effectiveness of High-Performance Concrete Jacketing in Improving the Performance of RC Structures. *Appl. Sci.* **2025**, *15*, 11421. [CrossRef]
38. Bayraktar, A.; Altunisik, A.C.; Türker, T.; Karadeniz, H.; Erdogdu, S.; Angin, Z.; Özsahin, T.S. Structural performance evaluation of 90 RC buildings collapsed during the 2011 Van, Turkey, earthquakes. *J. Perform. Constr. Facil.* **2015**, *29*, 04014177. [CrossRef]
39. Caglar, N.; Vural, I.; Kirtel, O.; Saribiyik, A.; Sumer, Y. Structural damages observed in buildings after the January 24, 2020 Elazığ-Sivrice earthquake in Türkiye. *Case Stud. Constr. Mater.* **2023**, *18*, e01886. [CrossRef]

40. Ozmen, H.B.; Inel, M.; Cayci, B.T. Engineering Implications of the RC Building Damages after 2011 Van Earthquakes. *Earthq. Struct.* **2013**, *5*, 297–319. [CrossRef]
41. Atmaca, B.; Demir, S.; Günaydın, M.; Altunışık, A.C.; Hüsem, M.; Ateş, Ş.; Angın, Z. Lessons Learned from the Past Earthquakes on Building Performance in Turkey. *J. Struct. Eng. Appl. Mech.* **2020**, *3*, 61–84. [CrossRef]
42. Yakut, A.; Sucuoğlu, H.; Binici, B.; Canbay, E.; Donmez, C.; İlki, A.; Ay, B.Ö. Performance of Structures in İzmir after the Samos Island Earthquake. *Bull. Earthq. Eng.* **2022**, *20*, 7793–7818. [CrossRef] [PubMed]
43. Altunişik, A.C.; Atmaca, B.; Kartal, M.E.; Günaydin, M.; Demir, S.; Uluşan, A. Assessment of structural damage following the October 30, 2020 Aegean Sea Earthquake and Tsunami. *J. Earthq. Tsunami* **2021**, *15*, 2150029. [CrossRef]
44. Cenan Mertol, H.; Tunc, G.; Akis, T. A site survey of damaged RC buildings in İzmir after the Aegean sea earthquake on October 30, 2020. *Građevinar* **2023**, *75*, 451–470. [CrossRef]
45. Ozturk, M.; Arslan, M.H.; Korkmaz, H.H. Effect on RC buildings of 6 February 2023 Turkey earthquake doublets and new doctrines for seismic design. *Eng. Fail. Anal.* **2023**, *153*, 107521. [CrossRef]
46. İnce, O. Structural damage assessment of reinforced concrete buildings in Adıyaman after Kahramanmaraş (Türkiye) Earthquakes on 6 February 2023. *Eng. Fail. Anal.* **2024**, *156*, 107799.
47. Yuzbasi, J. Post-earthquake damage assessment: Field observations and recent developments with recommendations from the Kahramanmaraş earthquakes in Türkiye on February 6th, 2023 (Pazarcık M7.8 and Elbistan M7.6). *J. Earthq. Eng.* **2024**, *29*, 3367–3392. [CrossRef]
48. Akar, F.; Işık, E.; Avcil, F.; Büyüksaraç, A.; Arkan, E.; İzol, R. Geotechnical and Structural Damages Caused by the 2023 Kahramanmaraş Earthquakes in Gölbaşı (Adıyaman). *Appl. Sci.* **2024**, *14*, 2165. [CrossRef]
49. Peker, F.Ü.; Yuzbasi, J.; Işık, E.; Büyüksaraç, A.; Avcil, F. Damage assessment, regional ground motion record evaluation, and seismic performance analysis of a high-rise 14-story dual system building after the 2023 Kahramanmaraş earthquakes. *Structures* **2025**, *80*, 109897. [CrossRef]
50. Kırtel, O.; Aydın, F.; Boru, E.; Toplu, E.; Aydın, E.; Sarıbıyık, A.; Ceyhunlu, A.I. Seismic damage assessment of under-construction industrial buildings: Insights from the february 2023 Türkiye-Syria earthquakes. *Case Stud. Constr. Mater.* **2024**, *21*, e03507. [CrossRef]
51. Altunsu, E.; Güneş, O.; Öztürk, S.; Sorosh, S.; Sarı, A.; Beeson, S.T. Investigating the Structural Damage in Hatay Province after Kahramanmaraş-Türkiye Earthquake Sequences. *Eng. Fail. Anal.* **2024**, *157*, 107857. [CrossRef]
52. Işık, E.; Radu, D.; Harirchian, E.; Avcil, F.; Arkan, E.; Büyüksaraç, A.; Hadzima-Nyarko, M. Failures in Reinforced-Concrete Columns and Proposals for Reinforcement Solutions: Insights from the 2023 Kahramanmaraş Earthquakes. *Buildings* **2025**, *15*, 1535. [CrossRef]
53. Yön, B.; Dedeoğlu, İ.Ö.; Yetkin, M.; Erkek, H.; Calayır, Y. Evaluation of the seismic response of reinforced concrete buildings in the light of lessons learned from the February 6, 2023, Kahramanmaraş, Türkiye earthquake sequences. *Nat. Hazards* **2024**, *121*, 873–909. [CrossRef]
54. Vuran, E.; Serhatoğlu, C.; Timurağaoğlu, M.Ö.; Smyrou, E.; Bal, İ.E.; Livaoğlu, R. Damage observations of RC buildings from 2023 Kahramanmaraş earthquake sequence and discussion on the seismic code regulations. *Bull. Earthq. Eng.* **2024**, *23*, 1153–1182. [CrossRef]
55. Sezgin, S.K.; Sakcalı, G.B.; Özen, S.; Yıldırım, E.; Avcı, E.; Bayhan, B.; Çağlar, N. Reconnaissance report on damage caused by the February 6, 2023, Kahramanmaraş Earthquakes in reinforced-concrete structures. *J. Build. Eng.* **2024**, *89*, 109200. [CrossRef]
56. İnce, E.G. Seismic performance of RC buildings with one-way joist slab: Insights from the 2023 Kahramanmaraş earthquakes. *Struct. Concr.* **2026**, *27*, 2147–2157.
57. Ministry of Public Works and Settlement. *Turkish Seismic Design Code (TSDC-2007)*; Ministry of Public Works and Settlement: Ankara, Türkiye, 2007.
58. AFAD. *Turkish Building Earthquake Code (TBEC-2018)*; T.C. Presidency of Disaster and Emergency Management Authority: Ankara, Turkey, 2018.
59. Çolakoğlu, H.E. Betonarme kolonların deprem performansında enine donatı aralığı etkisinin sayısal olarak incelenmesi. *Adıyaman Univ. J. Sci.* **2020**, *7*, 1–13. [CrossRef]
60. Atar, M.; İnce, O.; Taş, Ö.F.; Özmen, A.; Sayın, E. 6 Şubat 2023 Kahramanmaraş Depremleri Sonrasında Betonarme Kolonlarda Enine Donatı Kusurlarının İncelenmesi. *Fırat Univ. J. Eng. Sci.* **2024**, *36*, 221–230.
61. Merter, O.; Uçar, T. Betonarme kesitlerin doğrusal elastik ötesi davranışında tüketilen enerjiye boyuna donatı oranının, enine donatı aralığının ve eksenel yükün etkisi. *Niğde Ömer Halisdemir Univ. J. Eng. Sci.* **2015**, *4*, 21–39.
62. Taşkin, M.; Okay, F. Sargılama tipinin deprem yüklerine maruz kalan kolonların davranışına etkisinin sayısal olarak modellenmesi. *J. Eng. Sci. Des.* **2019**, *7*, 205–210. [CrossRef]
63. İnel, M.; Bilgin, H.; Özmen, H.B. Orta Yükseklikteki Betonarme Binaların Deprem Performanslarının Afet Yönetmeliğine Göre Tayini. *Pamukkale Univ. J. Eng. Sci.* **2007**, *13*, 81–89.

64. Işık, E. Investigation of the contribution of the reinforcement tie to the seismic behavior of reinforced-concrete columns. *Bitlis Eren Univ. J. Sci. Technol.* **2022**, *12*, 21–26.
65. İnel, M.; Bilgin, H.; Özmen, H. Performance of mid-rise reinforced concrete buildings during recent earthquakes in Turkey [Orta yükseklikli betonarme binaların Türkiye'de yaşanan son depremlerdeki performansı]. *Tek. Dergi* **2008**, *19*, 4319–4331.
66. Fortney, P.J.; Rassati, G.A.; Shahrooz, B.M. Investigation on effect of transverse reinforcement on performance of diagonally reinforced coupling beams. *ACI Struct. J.* **2008**, *105*, 781–788. [CrossRef]
67. Ding, Y.; Zhou, Z.; Wei, Y.; Huang, Y.; Tian, H. Axial compressive behavior of ultra-high performance concrete confined by high-strength transverse reinforcements. *Constr. Build. Mater.* **2022**, *324*, 126518. [CrossRef]
68. Mangalathu, S.; Shin, H.; Choi, E.; Jeon, J.S. Explainable machine learning models for punching shear strength estimation of flat slabs without transverse reinforcement. *J. Build. Eng.* **2021**, *39*, 102300. [CrossRef]
69. Tripathi, M.; Dhakal, R. Designing and detailing transverse reinforcement to control bar buckling in rectangular RC walls. *Bull. N. Z. Soc. Earthq. Eng.* **2021**, *54*, 228–242. [CrossRef]
70. Colajanni, P.; Pagnotta, S.; Recupero, A.; Spinella, N. Shear resistance analytical evaluation for RC beams with transverse reinforcement with two different inclinations. *Mater. Struct.* **2020**, *53*, 18. [CrossRef]
71. Sucharda, O. Identification of fracture mechanic properties of concrete and analysis of shear capacity of reinforced concrete beams without transverse reinforcement. *Materials* **2020**, *13*, 2788. [CrossRef] [PubMed]
72. Goharrokhi, A.; Ahmadi, J.; Shayanfar, M.A.; Ghanooni-Bagha, M.; Nasserasadi, K. Effect of transverse reinforcement corrosion on compressive strength reduction of stirrup-confined concrete: An experimental study. *Sādhanā* **2020**, *45*, 49. [CrossRef]
73. Valente, M. Seismic Protection of R/C Structures by a New Dissipative Bracing System. *Procedia Eng.* **2013**, *54*, 785–794. [CrossRef]
74. Fakharifar, M.; Sharbatdar, M.K.; Lin, Z.; Dalvand, A.; Sivandi-Pour, A.; Chen, G. Seismic Performance and Global Ductility of RC Frames Rehabilitated with Retrofitted Joints by CFRP Laminates. *Earthq. Eng. Eng. Vib.* **2014**, *13*, 59–73. [CrossRef]
75. Valente, M.; Milani, G. Alternative Retrofitting Strategies to Prevent the Failure of an Under-Designed Reinforced Concrete Frame. *Eng. Fail. Anal.* **2018**, *89*, 271–285. [CrossRef]
76. Sousa, I.; Peres, R.; Couto, R.; Bento, R.; Castro, J.M. Numerical Modelling and Damage Assessment Criteria for FRP-Retrofitted RC Columns. *Buildings* **2025**, *15*, 188. [CrossRef]
77. Ergin, K.; Güçlü, U.; Uz, Z. *A Catalogue of Earthquakes of Turkey and Surrounding Area (11 A.D. to 1964 A.D.)*; Maden Fakültesi Arz Fiziği Enstitüsü Yayınları: İstanbul, Turkey, 1967; Volume 24, p. 169.
78. Över, S.; Özden, S.; Yılmaz, H. Late Cenozoic stress state distributions along the Karasu Valley, SE Turkey. *Tectonophysics* **2004**, *380*, 43–68.
79. Alkan, H.; Büyüksaraç, A.; Bektaş, Ö.; Işık, E. Coulomb stress change before and after 24.01.2020 Sivrice (Elazığ) Earthquake (Mw=6.8) on the East Anatolian Fault Zone. *Arab. J. Geosci.* **2021**, *14*, 2648. [CrossRef]
80. Işık, E.; Harirchian, E.; Büyüksaraç, A.; Levent Ekinci, Y. Seismic and Structural Analyses of the Eastern Anatolian Region (Turkey) Using Different Probabilities of Exceedance. *Appl. Syst. Innov.* **2021**, *4*, 89. [CrossRef]
81. AFAD-TADAS. Disaster and Emergency Management Presidency, Department of Earthquake, Turkish Accelerometric Database and Analysis System. 2023. Available online: https://tadas.afad.gov.tr/ (accessed on 20 May 2026).
82. USGS. M 7.8—Pazarcik Earthquake, Kahramanmaraş Earthquake Sequence. 2023. Available online: https://earthquake.usgs.gov/earthquakes/eventpage/us6000jllz/executive (accessed on 20 May 2026).
83. AFAD. Türkiye Deprem Tehlike Haritaları. 2025. Available online: https://tdth.afad.gov.tr (accessed on 18 February 2026).
84. Işık, E.; Harirchian, E.; Bilgin, H.; Jadhav, K. The effect of material strength and discontinuity in RC structures according to different site-specific design spectra. *Res. Eng. Struct. Mater.* **2021**, *7*, 413–430. [CrossRef]
85. Doğan, G.; Ecemiş, A.S.; Korkmaz, S.Z.; Arslan, M.H.; Korkmaz, H.H. Buildings damages after Elazığ, Turkey earthquake on January 24, 2020. *Nat. Hazards* **2021**, *109*, 161–200. [CrossRef]
86. Seismosoft. SeismoStruct 2025—A Computer Program for Static and Dynamic Nonlinear Analysis of Framed Structures. 2024. Available online: http://www.seismosoft.com (accessed on 18 February 2026).
87. Işık, E.; Kutanis, M.; Bal, I.E. Displacement of the Buildings According to Site-Specific Earthquake Spectra. *Period. Polytech. Civ. Eng.* **2016**, *60*, 37–43. [CrossRef]
88. Işık, E.; Kutanis, M. Determination of Local Site-Specific Spectra Using Probabilistic Seismic Hazard Analysis for Bitlis Province, Turkey. *Earth Sci. Res. J.* **2015**, *19*, 129–134. [CrossRef]
89. *EN 1998-3*; Eurocode 8: Design of Structures for Earthquake Resistance-Part 3: Assessment and Retrofitting of Buildings. European Committee for Standardization: Brussels, Belgium, 2005.
90. Antoniou, S.; Pinho, R. *SeismoStruct-Seismic Analysis Program by Seismosoft; Technical User Manual*; Seismosoft: Pavia, Italy, 2003.